Determination of G-protein-coupled receptor oligomerization by molecular brightness analyses in single cells

Işbilir A., Serfling R., Möller J., Thomas R., De Faveri C., Zabel U., Scarselli M., Beck-Sickinger A.G., Bock A., Coin I., Lohse M.J., Annibale P.

Nature Protocols
2021 MAR ; 16(3): 1419-1451
2021 JAN 29 (first published online: final version)
doi: 10.1038/s41596-020-00458-1

URL: https://www.nature.com/articles/s41596-020-00458-1

Publisher: Nature Research (Springer Nature)

Determination of G-protein-coupled receptor oligomerization by molecular brightness analyses in single cells

Ali Isbilir[1,2], Robert Serfling[3], Jan Möller[1,2], Romy Thomas[1], Chiara De Faveri[3], Marco Scarselli[4], Annette G. Beck Sickinger[3], Andreas Bock[1], Irene Coin[3], Martin J. Lohse*[1,2,5], Paolo Annibale[1]*

1. Max Delbrück Center for Molecular Medicine, Berlin, Germany
2. Institute of Pharmacology and Toxicology, University of Würzburg, Germany
3. Institute of Biochemistry, Faculty of Life Sciences, University of Leipzig, Germany,
4. Department of translational research and new technologies in medicine and surgery, University of Pisa, Italy
5. ISAR Bioscience Institute, Munich, Germany

*correspondence to: m.lohse@mdc-berlin.de, paolo.annibale@mdc-berlin.de

EDITORIAL SUMMARY This protocol describes how to successfully design and execute molecular brightness analysis of GPCR oligomerization. Several labeling strategies, controls, and instructions for spatial and temporal brightness imaging and data analysis are provided.

TWEET A new Protocol for molecular #brightness analysis of #GPCR membrane protein #oligomerization in live cells.

COVER TEASER Brightness analysis of GPCR oligomerization

Abstract:

Oligomerization of membrane proteins has received intense research interest due to their importance in cellular signaling and the large pharmacological and clinical potential this offers. Fluorescence imaging methods are emerging as a valid tool to quantify membrane protein oligomerization at high spatial and temporal resolution. Here, we provide a detailed protocol for an image-based method to determine the number and oligomerization state of fluorescently labeled prototypical G protein-coupled receptors (GPCRs) based on small out of equilibrium fluctuations in fluorescence -i.e. molecular brightness- in single cells. The protocol provides a step by step procedure which includes instructions for (1) a flexible labeling strategy for the protein of interest (using fluorescent proteins, small self-labeling tags, or bio-orthogonal labeling) and the appropriate controls, (2) performing temporal and spatial brightness image acquisition on a confocal microscope and, (3) how to analyze and interpret the data excluding clusters and intensity hot-spots commonly observed in receptor distributions. ... Although specifically tailored for GPCRs, this protocol can be applied to diverse classes of membrane proteins of interest. The complete protocol can be implemented in one month.

Introduction

Membrane proteins play essential roles in controlling cell structure and function, including cell motility and movements, signaling, and metabolism. They often do so by linking the external environment with the cell interior[1]. While initially the cell surface and its constituents

have been considered quite static, many lines of evidence have revealed that the cell surface is a highly dynamic space, and that proteins at the cell surface are often highly mobile and show many types of interactions with each other [2]. Such interactions, falling under the broader notion of oligomerization, can be short-lived or stable, and the study of their mechanisms, characteristics and consequences has gained increasing attention since about forty years [3 4].

G-protein-coupled receptors (GPCRs) are a major class of membrane proteins that relay extracellular stimuli, such as hormones or neurotransmitters, into intracellular signals by activation of heterotrimeric G proteins [5]. Given their abundance and ubiquitous expression, they modulate almost every physiological process and represent the most popular class of drug targets [6]. GPCRs show multiple interactions among themselves as well as with other proteins. Several classifications of the superfamily of GPCRs have been proposed. The most widely used one divides them into five major families or classes [7]. Whereas class C GPCRs function as obligate dimers, both homo- and heterodimers [8], the situation for the much larger class A GPCRs is more complex and the impact of dimerization on their function is still not well understood. Although several examples of class A GPCRs have been shown to be fully functional as monomers [9], there are multiple lines of evidence proposing that class A GPCRs can also form dimers and sometimes even higher-order oligomers [10]. Since receptor dimerization may affect their localization, trafficking and signaling functions differently, it is important to rigorously assess the dimerization behavior in single living cells with appropriate methods. While functionally relevant GPCR oligomerization is a process that should occur at the plasma membrane, these proteins undergo very complex trafficking patterns, which can be reflected by retention in the Endoplasmic Reticulum, maturation in the Golgi or transport along cytoskeleton structures[11]. All these phenomena can affect the proper microscopic readout of oligomerization and require a method capable of discriminating them from bona-fide oligomerization occurring at the plasma membrane.

Here we describe a fluorescence-imaging based protocol for the systematic study of GPCR dimerization and oligomerization in live cells[12-14]. Our protocol relies on the detection of fluorescence fluctuations that are used to extract an average feature of the individual protein complexes (known as molecular brightness) and allows to calculate their oligomerization and local concentration. In spite of the broad range of interactions made by GPCRs, our approach remains essentially the same and can therefore be extended to studying any type of GPCR and other types of membrane proteins.

Development of the protocol

Over the years, we have used a variety of methods to determine the oligomerization state of GPCRs. Among these methods, we have found that those based on the measurement of molecular brightness are both reliable and straightforward [15,16]. Molecular brightness originates from the small out of equilibrium fluctuations of fluorescent particles diffusing in and out of a confocal excitation volume. The variance in the number of photons detected at different time intervals in individual pixels (Temporal Brightness), or equivalently, in different positions of the same -at equilibrium- region (Spatial Brightness), contains information on the intrinsic photon output of the individual fluorophore (i.e. the number of photons per fluorescent molecule collected during the exposure time), which defines the molecular brightness[16]. The observed brightness can be used to quantitate molecular oligomerization, since a fluorescent oligomer will have a photon output linearly dependent on the number of its labeled protomers. We have therefore used this approach to investigate the oligomeric arrangement of a set of GPCRs, including the well-studied β_1- and β_2-adrenergic receptors (β-AR), μ-opioid receptor (μ-OR), C-X-C Chemokine Receptor Type 4 (CXCR4) as well as the class B corticotropin release factor receptor 1 (CRF_1R)[12-14,17]. Although oligomerization

studies for these receptors, in particular the β_2-AR, have been performed for many years, results are conflicting [18] [19]. We reasoned that method-specific challenges, as well as the ability to effectively label these receptors may have been some of the potential confounding factors.

Since any optical method will benefit from a uniform and quantitative (maximal) fluorescent labelling of the target protein, we first systematically explored different labeling strategies. We observed that both fluorescent protein-labels, self-labeling tags (e.g. SNAP) as well as minimally perturbative bio-orthogonal labeling (i.e. by incorporating unnatural amino acids) allow quantitative receptor labeling and successful brightness determination [14] [20] [21]. Using each labeling strategy, we then developed a set of appropriate monomer and dimer controls in order to carry out molecular brightness experiments.

The implementation of successful molecular brightness experiment requires special attention to several key experimental settings: this ultimately boils down to ensure that the system observed is at any time in thermodynamic equilibrium, with fluorescence fluctuations arising only from protein diffusion within the plasma membrane and not from other sources, such as receptor trafficking, macroscopic motions of the cell membrane, formation and diffusion of vesicles, etc. In particular, we recently determined how the acquired data should be analyzed to selectively extract information on receptor oligomerization only at the cell surface and simultaneously avoid artifacts due to the intracellular expression of the protein [12]. Using this strategy, we could quantitatively determine the agonist-dependent oligomerization state of the μ-OR, or the inverse agonist dependence of the CXCR4 oligomerization through side-by-side single particle tracking and molecular brightness analysis[13,17].

Overview of the procedure

This protocol provides a comprehensive pipeline to establish an oligomerization assay, from initial generation of cell lines expressing the fluorescently-labelled receptor of interest, to data acquisition, analysis and interpretation (**Figure 1**). First, the receptor of interest has to be fluorescently labelled, commonly by fusion to a fluorescent tag. Multiple labeling strategies are available, ranging from C-terminal fluorescent protein tags [22-24](Step 1 Option A), N-terminal SNAP-tags [25] (Step 1 Option B) to non-canonical amino acids covalently labeled with organic fluorophores [26] (Step 1 Option C). Example results obtained using these diverse labeling strategies are displayed in **Figure 2**. Step 1 also illustrates the molecular cloning steps necessary to generate plasmid DNA for the expression of the receptor of interest and the relevant controls (**Figure 3**). Sample preparation, ranging from cell culture to labeling -depending on the chosen labeling strategy is then addressed in step 2 (Option A for C-terminal fluorescent protein tags and SNAP-tags, Option B for non canonical amino acid labeling).

Next, we describe how to image cells expressing the labeled receptor of interest and how to acquire movies and/or snapshot images in the confocal microscope using two independent strategies, namely temporal brightness (Steps 3-9 Option A) and spatial brightness (Steps 3-9 Option B). The key steps associated to data acquisition and analysis for the two approaches are displayed in **Figures 4-5**. For each of the two strategies, we discuss the critical step of area selection to obtain oligomerization information only from homogeneous (=in equilibrium) regions of the plasma membrane by means of quantitative area selection (Steps 10-12, Option A for temporal brightness, option B for spatial brightness) (**Figure 6**)[12]. The results from the two independent strategies are then combined to provide a robust map of the receptors' oligomerization state as well as for their plasma membrane concentration (Steps 13-14) (**Figure 7A-B**). In addition, we provide a tool to quantify the labeling efficiency of receptors labeled with fluorescent proteins or after incorporating unnatural amino acids (Box 1) (**Figure 8A-B**).

Recent high-quality protocols on brightness analysis have dealt with specific and advanced aspects of the data processing [27]. Therefore, we aim here to provide a more general description, covering the entire process of experimental data acquisition and analysis, from sample preparation to final data analysis. We designed our protocol such that it is amenable to virtually any labeling strategy, ranging from intracellular fluorescent protein fusion tags to extracellular labeling of non-canonical amino-acids. The imaging steps of our protocol refer to a specific confocal setup (Leica SP5/8), but the protocol is broadly applicable on other setups as well, and we provide some general hints for detector calibration in Box 2. In addition, we provide a standard set of controls, fully validated, that are required as references in any quantitative study of GPCR oligomerization.

Applications of the method

This protocol provides a step by step approach for quantitative analysis of membrane protein oligomerization and concentration. Because our approach is image-based, the protocol is robust at assessing local differences, and provides multiple analysis possibilities (i.e. excluding or including heterogeneities) depending on the biological concept that is studied.

The protocol will be valuable for scientists with questions related to the quantification and oligomerization of membrane protein under diverse biological states (e.g. effect of drugs, in the context of specific mutations, following activation of distinct pathways, during cell migration and morphological changes, etc.). Some of the functional roles of receptor oligomerization are nicely reviewed in [4]. About 30% of the proteins found in *Homo sapiens* are expected to represent integral membrane proteins [28], meaning that the membrane proteins under investigation can range from immune receptors [29] to GPI anchored proteins [30], or receptor tyrosine kinases [31]. Moreover, some general concepts can be extended to oligomerization studies of non-membrane proteins in any other cellular compartment, as illustrated by examples of nuclear actin [32] or cytosolic phosphodiesterases [33]. The main requirement is that a strategy for highly efficient and uniform fluorescent labeling is available. The broader application of the method has been limited, in our opinion, by the lack of a standard set of well-validated controls, a clear guide about receptor expression and labeling, and a clear protocol for data acquisition and analysis based on an open source analysis code. It is our aim to provide all of these here and make them available to interested scientists.
...

Comparison with other methods

A broad range of distinct approaches has been used in the analysis of membrane protein oligomerization in general and specifically for GPCRs, comprising both biochemical and biophysical (mostly optical) methods.
Originally, biochemical approaches such as SDS-Page or co-IP were employed to identify receptor dimers and oligomers (for a review we refer the reader to [34]). Molecular biology strategies combined with radioligand binding assays were able to provide the first evidences of receptor heteromerization [35].

Since the first bioluminescence resonance energy transfer (BRET) investigations on the oligomerization behavior of the β_2-AR [18,36], a large number of studies have addressed the oligomerization state of GPCRs with fluorescence -as well as bioluminescence- resonance energy transfer approaches[10]. However, although there appears to be a consensus that GPCRs can form dimers, there remain some conflicting data on the extent and relevance of such dimers in cells. For example, by using the same method and the same receptor, for

BRET analysis of β_2-AR oligomerization, several reports support the presence of oligomers [18,37], while others suggest that these complexes are less abundant or even absent[19,38,39]. BRET is a powerful method that can also be used for the study of GPCR conformational transitions and cellular signaling [40-42]. It can also be employed to address the finer conformational transitions occurring at the level of an oligomeric assembly [43]. However, one of the main challenges is that BRET imaging (as well as epi-FRET) is unable to distinguish the oligomerization signal originating from the plasma membrane from that occurring in the cytosol. Considering the complex and dynamic trafficking patterns of most GPCRs [11], this may contribute to the high oligomerization states observed in several studies[18,37,39,44]. For this reason, quantitative FRET/BRET studies of membrane protein oligomerization, including GPCRs, should consider combining FRET/BRET with optical sectioning imaging approaches, such as confocal or total internal reflection fluorescence (TIRF)[45,46].
Although FRET and BRET differ in the use of a luminescent donor (BRET), activated by a substrate, rather than a fluorophore (FRET), both can be applied for oligomerization studies. In a microscope, FRET is usually preferred, while high throughput screening approaches make common use of BRET[47].

Among the most promising and accurate approaches developed over the last several years, single molecule tracking (SMT) has gained widespread attention in the field as it can provide information on oligomerization dynamics at the single receptor level, without the need for an ensemble average[48]. This has allowed substantial insight into the kinetics and prevalence of membrane receptor oligomers, including GPCRs [49-56]. The major limitation of the method is the assessment of oligomerization at the plasma membrane when the receptor concentration exceeds a few molecules/μm^2 [51,55]. At concentrations above this value, individual molecular Point Spread Functions (PSFs) begin to overlap and accurate localization and tracking in living cells becomes not feasible. While endogenous GPCRs concentrations can fall within the single molecule regime[57], there are instances, for example, in certain cancer cells, where this threshold can be exceeded.[58]

In comparison to SMT methods, fluorescence fluctuation spectroscopy techniques offer a robust tool to investigate receptor dimerization at high, as well as lower expression levels. Lateral diffusion of the fluorescently labeled receptors generates fluctuations of the fluorescence signal within the observation volume. The observed fluorescence photon counts and their fluctuation can be directly related to the receptors number and their oligomerization state. This is achieved by computing the molecular brightness [15,16,59-63]. This family of methods, to which our approach belongs, has the advantage that it can be performed over a wide concentration range, requires straightforward data analysis (calculation of means and variances) and can be used with a large variety of dyes. Originally, single point Fluorescence Correlation Spectroscopy (FCS) measurements were used to provide histograms of the collected photons from a single PSF/pixel, the so-called Photon Counting Histogram (PCH) [15,64,65]. In principle, PCH measurement can be performed in multiple observation points/pixels within the cell, leading to a spatially resolved brightness assessment [66]. In order to do so, the number of PCH measurements would need to be as high as of the number of pixel of the desired *brightness image*. To obtain a 128x128 pixels map this would correspond to over 10^4 individual measurements.
Another strategy is to extend this approach directly to image-based acquisitions relying on the statistical analysis of many pixels (again of the order of 10^4), where fluctuations are either recorded over time (number and brightness (N&B)) [67] or space (SpIDA) [60]. This allows, among others, characterizing the oligomerization state of membrane receptors such as the GPI-anchored membrane receptor uPar [59], the ErbB [68] or more recently the FGFR2 [69]. We provide for the convenience of the reader a summary of some key molecular brightness methods and their application domains in Table 1.

The fundamental advantage of image-based brightness approaches is that a spatially resolved view of the plasma membrane allows researchers to discard regions where

receptor aggregation phenomena are not related to oligomerization, but rather to other trafficking processes (such as recruitment by endocytic machinery or retention in the endoplasmic reticulum), from the analysis [70,71]. Nevertheless, detailed reports on brightness analysis of GPCRs are still relatively scarce, and either focus on very specific applications (e.g. pharmacology of specific receptors, such as the serotonin 5-HT_{2C}, muscarinic acetylcholine M_1 receptors, metabotropic glutamate or μ-opioid receptors) [61,72,73] or on methodological advances of the method [12,14].

Limitations of the approach

There are three conceptual limitations to brightness analysis: (1) it is an ensemble average method, (2) it is not self-calibrating and (3) it is not high throughput.

Being a statistical method based on extracting average parameters (average number of molecules in the PSF/pixel and average brightness of the species diffusing) from small out of equilibrium fluctuations, brightness analysis classically provides a mean oligomerization indication [16]. As such, it is impossible to say if an individual molecule is at any time monomeric or oligomeric, as opposed to single molecule tracking strategies [13,54,55] Furthermore, since this approach yields the ensemble average, the underlying oligomeric equilibrium is unknown: e.g. a dimeric brightness may arise from constitutive dimers as well as from a monomer-trimer equilibrium, although more recent approaches have suggested data analysis strategies to deconvolve the oligomeric composition of the sample[27].

In contrast to BRET/FRET approaches, where the RET efficiency is an intrinsic reporter of the intermolecular distance between two molecules [18], absolute molecular brightness values extracted are influenced by a number of factors, ranging from quantum yield of the fluorophores (which can be affected by the imaging medium), appropriate focusing of the microscope at the plasma membrane (defocus will lead to loss of brightness), numerical aperture of the objective, stability of the laser power as well as more subtle effects such as alignment of the confocal pinhole or even temperature sensitivity of the photodetector (See Troubleshooting). Thus, brightness analyses provide relative values that require normalization to reference proteins. For this reason, we recommend frequently (ideally with every experiment) measuring cells expressing the appropriate monomer (and where possible, oligomeric) control. This can be used to normalize the brightness of each experiment to *fold of monomer value* or *oligomeric state* (as later shown in Figure 7B), allowing a more robust comparison of the brightness values across experiments [13,74]

Although more rapid compared to SMT, brightness analysis requires sample sizes of the order of tens of cells be screened. In this respect it does not compare to the throughput of plate reader assays or flow cytometry. Furthermore, our experience is that molecular brightness analysis can result into artifacts when used to study receptor oligomerization. Most prominently, the inclusion of fluctuations that are not related to molecular oligomerization at the membrane, but rather to trafficking of the receptor, seem to confound automatic image segmentation algorithms [12]. GPCR trafficking is a biologically important, sometimes quantitatively dominating, complex and continuous process: it is characterized by the formation of small aggregates into an endocytic pit, leading to very early endosomes, and then to more mature and dynamic endosomes. This makes discriminating a small oligomer from a receptor cluster in a very early endosome a challenging process [11]. However, the effect of these processes is distinct depending to the brightness method being used [12,60,75]. By combining temporal and spatial brightness analysis and offering an ample choice in labeling strategies, the present protocol is aimed at compounding as much as possible artifactual reading.

Experimental design

Selection of the desired labeling strategy for the GPCR of interest. Our protocol can be applied to any G protein-coupled receptor, as GPCRs share significant structural homology [76]. Four options are available for fluorescently tagging a GPCR in living cells [77-80]: (1) tagging with a fluorescent protein (Figure 2A-B), (2) labeling with self-labeling protein tags (Figure

2C), (3) labeling using a fluorescent ligand (Figure 2D) and, (4) bio-orthogonal labeling of incorporated non-canonical amino acids (Figure 2E-H). Over the years, our lab as well as others, has attempted all four strategies [13,14,81-83] (for a general recent review, we refer the reader to [49]). While specific labeling strategies may be required for specific spectroscopy techniques (e.g. long lifetime fluorescent ligands for time resolved FRET [82]or self-labeling protein tags for oligomerization assays using SMT [51]), molecular brightness approaches do not have any such requirement, provided that the fluorophore used has a detectable emission under the microscope and its labeling efficiency is high enough.

With the exception of using fluorescent ligands (the design of which would require a separate treatment and for which we refer to review articles such as [84]), all other approaches demand a rational decision about where to insert the label in the receptor using molecular cloning. As opposed to other approaches, fluorescent ligands provide the attractive option to be 'washable', that is they can be displaced by competition with an appropriate 'dark' ligand, allowing to reverse the labeling of the GPCR of interest (Extended Data Figure 1). After the first example of C-terminal labeling of a GPCR with GFP [22,23], direct GPCR labeling using fluorescent proteins has become widespread. GPCR labeling has therefore been classically demonstrated mostly C-terminally, but also N-terminally and in the extra- and intracellular loops (for a review see Bohme and Beck-Sickinger and references therein[77]). Ideally, when designing a novel labeled GPCR three key considerations have to be kept in mind: the inserted label should (1) not disrupt receptor signaling, (2) not disrupt receptor localization and (3) achieve high (ideally 100%) and uniform labeling efficiency. Where to insert the fluorescent tag is up to individual investigators after having examined these aspects and carefully screened the literature for the relevant GPCR. In this protocol we will provide examples based on our own laboratory experience concerning labeling the class A β_1-AR and β_2-AR, the μ-OR, the CXCR4 as well as the class B corticotropin releasing factor receptor 1 (CRF_1R).

Fluorescent protein labeling is the most widespread approach to label GPCRs. For class A GPCRs, GFP-like fluorescent protein tagging at the C-terminus of a GPCR is typically straightforward and mostly preserves the receptor's localization. However, since GPCR C-termini often contain sequences susceptible to phosphorylation by G protein-coupled receptor kinases (GRKs) or important for protein-protein interactions involved in receptor localization and trafficking[85], labelling at this location may alter the physiological receptor localization, and, in rare cases, signaling[86]. It is therefore important to validate any labelled GPCR variants for localization and function, as extensively discussed in the literature [14,40,83]. Furthermore, the addition of an intracellular protein of a molecular weight about one third of that of the GPCR may have unexpected consequences for receptor motility, as recently highlighted by rapid diffusion measurements [14]. We shall note here that although most GPCRs lack a proper 'signal peptide' targeting them to the plasma membrane [87], N-terminal GFP labeling may still hamper proper localization. Replacing the large GFP moiety with a much smaller N-terminal self-cleavable signal sequence of influenza hemagglutinin (MKTIIALSYIFCLVFA) followed by an epitope tag (i.e. FLAG-tag (DYKDDDDA) in this protocol) to facilitate immunostaining or Western blotting, usually solves this problem [81,88]. Intracellular loop labeling is possible, but large GFP-like fluorophores have been shown to disturb G-protein coupling and downstream signaling, a problem mostly obviated by the small FlAsH-tetracysteine system [83]. We summarize in our procedure under step 1, Option A the molecular cloning steps necessary to achieve both N- and C-terminal labeling of the prototypical GPCR β_2-AR, as a reference example.

Taking into account that the molecular weight of self-labeling protein tags is comparable to that of GFP, most considerations discussed for fluorescent protein labeling apply also here. The advantage of this strategy is the possibility of choosing organic fluorophores of many colors and improved photostability and brightness, covalently fused to a chemical group which is then recognized and covalently bound by the protein tag [25,89,90]. N-terminal labeling

is favored given the ability to use membrane-impermeable dyes, reducing the nonspecific signal due to retention of the fluorophore in the cell cytosol. This approach has been applied successfully to GPCRs for a number of applications, ranging from FRET to single molecule tracking [51,91]. Step 1, Option B highlights the exemplary cloning step to obtain an N-terminally labeled SNAP-β_2-AR

The incorporation of non-canonical amino acids (ncAAs) into GPCRs via the genetic code expansion technology offers an alternative approach, which has the advantage that it allows for installing small, bright, and photostable organic fluorophores onto GPCRs by modifying only one single amino acid. In this protocol, we exclusively focus on the orthogonal amino-acyl-tRNA-synthetase/suppressor tRNA pair *Mb*PylRS^{AF}/tRNA^{M15} to incorporate the ncAA *trans*-cyclooct-2-ene lysine (TCO*K) into proteins in mammalian cells[92]. Based on ultra-fast click-chemistry, TCO*K reacts in a few minutes at room temperature with commercially-available tetrazine conjugated dyes. Due to the small size of the probe it is in principle possible to label GPCRs at every solvent-accessible epitope both at the extracellular and intracellular side. However, as some extracellular epitopes have been shown to be important for ligand binding and receptor activation, a preselection of suitable positions for ncAA incorporation can be made based on mutagenesis data available in the GPCR database [93] [80]. The use of membrane impermeable fluorescent dyes further favors specificity of membrane labeling, whereas membrane permeable dyes require more extensive washout steps. Step 1, Option C describes how to clone a TCO*GPCR mutant, such as the TCO*M_2R.

As a general note for all above options, once transient transfection (discussed in this protocol) of the construct of interest proves satisfactory, we recommend where possible to create stably expressing or gene-edited cell lines, which will express the protein at (near-)physiological levels and ensure stoichiometric protein tagging in the case of gene-edited cell lines.

Preparation of the appropriate controls. In our approach fluctuations in fluorescence levels in the confocal excitation volume (Figure 1, Steps 3-9) are used to determine a molecular brightness. If a receptor rapidly diffuses through the excitation volume, only few photons are detected during one exposure time, whereas more photons are detected from a slowly diffusing receptor. It is however important to consider that the detected photon output of a fluorophore depends on a large number of factors, such as the Numerical Aperture of the objective lens, the laser power used, the excitation wavelength and the detection window. This means that molecular brightness is not an absolute property of the fluorophore (in contrast to the extinction coefficient and the quantum yield), and any measurement needs to be calibrated to a reference control imaged under the same conditions as the sample (see “Limitations of the Approach”).

The control receptor should be a species whose oligomerization state is precisely known, which carries the exact same protein tag and/or fluorescent label as the GPCR of interest, and that has a similar diffusion rate and type of motion (e.g. diffusive vs sub-diffusive) with the receptor of interest (Figure 3A). Based on our findings, the β_1-AR under basal conditions displays a remarkable monomeric fingerprint [13,51,81,94], making it an ideal monomeric control. The receptor is amenable to fluorescent labelling by using N- or C-terminal monomeric EYFP fluorescent protein tags (Figure 2A) (Step 1, Option A) or N-terminal SNAP-tag labeling (Figure 2C) (Step 1, Option B). While a fluorescent monomer control is strictly necessary to calibrate any brightness experiment, a fluorescent dimer (i.e. a protein carrying twice the fluorophores of the monomer, therefore yielding double brightness) is also helpful to place experimental data in the right context. To this aim, we have fused a tandem EYFP tag (2xEYFP) to the β_1-AR. To avoid artifacts such as potential energy transfer between the two EYFPs and to preserve the precise two-times EYFP brightness value, we inserted a single alpha helical linker (A(EAAAK)$_4$A) between the two EYFPs [95]When imaged by

temporal brightness, the labelled receptor displays a brightness value in agreement with the expected value twice of that observed for single EYFP (Figure 3B) (Step 1,Option A).

A further advantage offered by molecular brightness approaches is the possibility to use partial photobleaching to obtain information regarding the mono-/oligomeric state of a receptor. If a receptor is monomeric, photobleaching of a subset of the fluorophores will still lead to a monomeric population, just with a reduction of the number of emitters. Since the molecular brightness is a property of the individual emitter, the molecular brightness remains unchanged. On the other hand, if a receptor is dimeric and a fraction of the fluorophores is bleached, this results in a number of dimers containing only one label. In brightness terms these *protein dimers* will now effectively appear as *fluorescence monomers.* Step 9 Options A and B describe how to perform photobleaching in the context of a brightness experiment. An example of this is highlighted in Figure 3B, where partial bleaching the β_1-AR-EYFP, maintains the same brightness level, whereas the partial bleaching of the β_1-AR-2xEYFP yields a sizable brightness reduction.

The same behavior can be observed when working with the SNAP-tagged version of the β_1-AR: upon partial bleaching the brightness remains the same (Figure 3C). This is in remarkable contrast to the behavior of another protein, oftentimes encountered as a monomeric control in the literature[96,97], namely the CD86. In our hands the N-terminally SNAP tagged CD86 [51] shows a non-negligible degree of oligomerization at the expression levels required for brightness analysis, which returns to baseline levels upon partial photobleaching. While the receptor has found its way and use, especially in the single molecule tracking field, as a monomer control [51], our data, as well as careful inspection of previous data available in the literature [51,81,98] seem to indicate non-negligible levels of oligomerization. The use of self-labeling tags such as SNAP-tags, or tags amenable to covalent bonding with organic dyes such as non-canonical amino acids, offer an additional attractive feature for molecular brightness experiments. By titrating the amount of labeling dye one can achieve such a low concentration of labeling with one dye, that the chance that two protomers part of a dimer are simultaneously labeled by the same fluorophore is exceedingly low (Step 2.VII Option B). Since a monomer cannot bear more than one fluorescent label, the apparent brightness B of the monomeric receptor is independent from the labeling stoichiometry. In contrast, a dimeric receptor sample can bear either one or two fluorescent labels, so that their brightness increases with increasing amounts of fluorescent label. When the labeling stoichiometry is very low, dimers will bear, if any, only one fluorescent label, thus yielding the brightness of a monomer. This information can be used to reference further measurements where labeling is performed at 100% [14]. We applied this strategy to a bioorthogonally labeled version of the CRF_1R, which bears TCO*K at position 263 (Figure 2G-H), and for which previous reports suggested the tendency to oligomerize [99,100]. From these experiments, we conclude that the CRF_1R is a dimer.

Confocal microscopy data acquisition and data analysis. Once the controls as well as the receptor of interest are prepared and transfected, and their expression and localization at the plasma membrane have been verified (Step 1.V Option A, Step 1.IV, Step 2.VIII Option A and Step 2.IX Option B), the molecular brightness can be determined. In this protocol we describe how to use a confocal microscope operating in photon-counting mode. Leica confocal microscopes provide this option. The key points of our protocol are ultimately not affected by the use of photon counting vs analog detectors. For confocal microscopes operating in analog mode the data acquisition procedure is the same, whereas the data analysis (Steps 3-9) should be adapted and the detector properly calibrated (See Box 2); we further refer the interested reader to more specialized publications [27,60,67,75]. In our protocol we focus on the basolateral membrane of cells expressing the GPCR of interest since it yields a larger number of data pixels and therefore a larger statistical sample. Other approaches have made use of the lateral membrane of cells [59,101]. The imaging guidelines described in this protocol refer to the use of a Leica SP8 confocal microscope, with a White

Light Laser (WLL) source and two GaAsP Hybrid Photomultiplier Detectors (HyD) (see Materials and equipment).

A few important considerations regarding image acquisition settings are important to take into consideration, regardless of the microscope being used. Brightness methods use small fluorescence fluctuations out of equilibrium to capture the molecular brightness. Depending on the characteristic diffusion time of the receptor or molecule of interest (see Extended Data Figure 2A), this sets an upper limit on the exposure time (or pixel dwell time) for a Temporal Brightness acquisition. This maximum exposure time is given roughly by $\tau_D = \frac{w_0^2}{4D}$, the diffusion time through the PSF, in which w_0 denotes its waist (0.3 μm is a good estimate in the visible range) and D denotes the diffusion coefficient of the species. For GPCRs, whose diffusion coefficient is of the order of 0.1 $\mu m^2/s$ [52,64], this means that the exposure time should be lower than about 200 ms. Since the $\boldsymbol{\tau}_D$ is the time when the signal begins to decorrelate, since the molecule diffuses out of the PSF (Extended Data Figure 2A), it is advised to work with at least 10 times shorter exposure times than $\boldsymbol{\tau}_D$. Depending on the confocal microscope used, the pixel dwell time can be used to set the frame time, or, as in Leica microscope, the line scan rate determines the dwell time. In general, exposures times of the order of a few to tens of μs are fine for detecting fluctuations originating from membrane proteins. On the other hand, the interval between the frames should be longer than $\boldsymbol{\tau}_D$, in order to allow different frames to sample distinct configurations of the thermodynamic ensemble. Longer dwell times would also be compatible with the requirements outlined in Extended Data Figure 2A, but would lead to unreasonably long acquisition times, which can result in extensive photobleaching and sample drift/movement. Photobleaching is also the main concern when setting the laser power. Higher laser powers will increase the brightness and the overall signal to noise ratio, but will also increase bleaching. It is important to note that a bleaching sample contains extra variance due to slow fluorescence decay, which will combine with the variance due to molecular diffusion and ultimately affects the brightness readout. Since sample bleaching depends on many parameters, including but not limited to the microscope settings. In general, we recommend to set a laser power value which yields an overall bleaching below 10% over the course of the acquisition, and work at that power level or below. Finally, also sample stability is important, and where possible a hardware autofocus (i.e. non-image based) should be employed. In addition, detrending algorithms which remove slow fluctuations from the sample can be employed, such as a boxcar filter[102] (Step 9.III Option A).

Imaging of live single cells results in a map of the photon counts in different pixels of an image and over time. The fluctuations in the photon counts collected from each pixel reflect the number distribution of the receptors in the pixel (determined by diffusion), as well as the noise of the photon detection (shot noise). As anticipated, the sample under investigation -in this case the cell membrane- needs to be as close as possible to thermodynamic equilibrium. This means that the fluctuations in the photon counts have to be generated only by molecular diffusion of the GPCRs and that all other sources of fluctuations must be minimized: cells need to display a homogeneous membrane devoid, as much as possible of ruffles or cellular processes such as filopodia (See Figure 1, Step 8 and Figure 4B). Resting, unstimulated cells are favored over motile cells (unless specifically studying the role of a protein in cell motility). Cells need to be imaged at relatively low confluence and isolated, to avoid overlap between membranes of multiple cells (Step 8). For our studies we observed that resting HEK293AD cells meet these criteria. However, experiments in other cell lines were also successfully conducted [13].

Temporal Brightness (Step 9 Option A) measures the fluctuations of photon counts in each pixel as a function of time, allowing to calculate a brightness value from the variance and mean of this time series (Figure 4A). This is achieved by collecting a movie containing a number of frames equal to the number of temporal data points which will then be required to

calculate mean (k) and variance (σ): typically, 50-100 frames are sufficient. As a result, a new brightness image can be constructed, where each pixel displays its apparent brightness value in a false color scale (Figure 4B). The so-called apparent brightness (B) in each pixel can be determined from using the following formula (See also Box 2):

$$B = \frac{\sigma^2}{k} = \varepsilon + 1$$

where ε is the actual molecular brightness (photons/molecule/exposure time), σ indicates the standard deviation of the signal and k indicates its average value. Intensity counts due to immobile proteins yields by definition a σ^2/k ratio equal to 1, and therefore do not contribute to the molecular brightness [67]. Fluctuations due to slowly moving aggregates or cell features can be filtered out using basic detrending algorithm (Dalal et al., 2008). The values from each pixel of a selected region (see "selecting the area of interest" below, Step 12 Option A) of the membrane are then averaged to provide a histogram of the brightness values (one occurrence for each pixel). The peak of the histogram or the average brightness of the region of interest can be used for to obtain a molecular brightness value from the selected region [59,62,67] (Figure 4C). Temporal brightness values for each pixel are conventionally displayed as B vs intensity scatter plots. In this case, regions of similar expression and oligomerization show up as clusters in the plot. Figure 4E displays the scatter plot associated to Figure 4C-D. The two clusters, highlighted as F and G correspond to the pixels highlighted in white in Figure 4F and Figure 4G respectively. The average intensity image from the Temporal Brightness movie in Figure 4H illustrates an alternative selection mode, based upon choosing a region in the intensity picture. This type of representation allows for a flexible data analysis strategy: pixels can be grouped, and their brightness extracted based on their intensity, spatial location, brightness similarity, or a combination of these properties.

Spatial Brightness (Step 9 Option B) measures the fluctuations of photon counts across pixels of the same image. If each pixel is considered as an independent observation spot, there is a clear conceptual analogy to the temporal brightness approach, although this time the variance in the signal arises from the pixel to pixel comparisons within the same confocal image rather than from multiple snapshots (Figure 5A). Upon area selection (Figure 5B-C), a histogram of the intensity values from the region of interest (ROI) can be calculated (Figure 5E), and the associated variance and mean can be used to calculate a brightness value according to the same formula used for the Temporal Brightness calculations. This approach is distinct from Spatial-Temporal correlation Spectroscopy methods, such as RICS, which use a single image to extract the diffusion rate of the species under investigation [103]. In the case of Spatial Brightness, local aggregates or inhomogeneities in receptor spatial arrangement can contribute, if included in the selection, to the variance and therefore to the measured brightness. We show here the exemplary case of β_1-AR -EYFP and β_1-AR -2xEYFP, the latter before and after partial photobleaching (Step 9.IV Option B). The resulting number and brightness values are reported in the table of Figure 5E.

Selecting the area of interest. One key aspect of the brightness data analysis is the selection of homogeneous regions of the plasma membrane that satisfy the condition of thermodynamic equilibrium (Step 12). Plasma membranes are far from homogeneous and many of their properties can confound a brightness measurement. Spatial inhomogeneities show up differently in the two approaches used (spatial and temporal brightness). Hence, a robust molecular brightness measurement should encompass always both [12]. An example is a static endosome, containing many labeled receptors near the plasma membrane. This endosome (which will be visible as a hotspot in the intensity picture) will skew the spatial brightness measurements but not affect the temporal brightness measurement, since static features do not yield fluctuations in time. On the other hand, a dynamic endosome will yield a streak of high brightness points in a temporal brightness acquisition, as shown in Figure 4B.

In the literature, indications like “a homogeneous region was selected”, or “regions with inhomogeneous fluorescence intensity (ruffles, sites of endocytosis) were avoided” are often being used, but not further specified [12]. In this protocol we discuss step by step how to select a region of the plasma membrane devoid of hot-spots, clusters, or artifacts that may skew the molecular brightness reading, based on our recent findings [12]. In general, visual identification of a homogeneous region remains the starting point. Figure 6A shows a confocal picture of a cell expressing the β_1-AR -EYFP, localizing to the basolateral membrane of a HEK293-AD cell, acquired in a spatial brightness experiment. Data obtained from a good and a bad selection of the ROI are displayed. The ‘bad’ choice (blue histogram in Figure 6B) corresponds to a ROI containing a number of bright hot-spots, leading to a histogram which is broader, resulting in higher brightness and lower number of molecules. In contrast, the neighboring ‘good’ ROI is more homogeneous and results in a narrower histogram, lower brightness and a higher number of molecules (Step 12). However, such qualitative strategy for selection has its limitations. In many cases, less obvious inhomogeneities may be harder see by eye. We therefore recommend to quantitatively score the distribution of pixel intensities of a selected ROI, in order to determine which one approximates better a Gaussian distribution, and is therefore closer to thermodynamic equilibrium. Figure 6C displays a simulated confocal snapshot, where ‘by definition’ two species diffuse in a monomer-dimer equilibrium having a resulting molecular brightness of 10. On top, a number of large arbitrarily shaped intensity hot-spots, unrelated to the monomer-dimer equilibrium, have been generated. Calculating the histogram of the whole image and using the mean and variance of the fitting Gaussian (Figure 6D) not only leads to a poor fitting, but also to an overestimation of the molecular brightness. The deviation of the experimentally observed distributions of intensity occurrences from a Gaussian can be quantified by using a Gaussianity test known as Kolmogorov-Smirnov test [104] . The test yields a distance between the two distributions, and a reference value. The ratio of the two can be used as a score. If equal to one or larger, the distribution is Gaussian; the lower the value, the poorer the approximation to a Gaussian (see 12.IV Option A and Step 12.III Option B).Once a ROI without hotspots is selected (Figure 6E), not only the distribution fits much better to a Gaussian, but also the Gaussianity score is now significantly higher. Furthermore, the recovered brightness (ε=(B-1)=10.5) is closer to the ‘true’ brightness of 10. We therefore advise to perform such tests upon ROI selection, before extracting molecular brightness values

Data display and interpretation. As we anticipated in the previous section, the combined use of spatial and temporal brightness is advantageous to properly identify the oligomeric state of the receptor, as they allow filtering out different types of artifacts. Nevertheless, even after appropriate ROI selection, background effects may still remain. For this reason, we recommend plotting the results of the two methods for the GPCR of interest, together with the monomeric (and possibly dimeric control), as displayed in Figure 7A (Steps 13-14). A line should connect the monomer and dimer controls, and the receptor of interest should be positioned along this line, its position depending on the degree of receptor oligomerization. Nevertheless, deviations from the line may reveal further insights into the dynamics and trafficking of the GPCR: notably, a higher temporal brightness than expected indicates the presence of dynamic trafficking, whereas higher spatial brightness may suggest small clustering (e.g. at the onset of endocytosis), which cannot be excluded by ROI selection. Once a monomer control has been adopted, such as β_1-AR in our case, all brightness values can be referred to an oligomeric state, e.g. a scale where one indicates monomer and two indicates dimer. As an example, we show data obtained with μ-OR, labeled either N-terminally with a SNAP-tag or C-terminally with an EYFP, in Figure 7B. Here the dimeric receptor CD28 is used as a dimer control [81]. In principle higher order oligomerization can be assessed, as long as appropriate controls (e.g. trimers, tetramers...) are generated and imaged. Although there is not a strict upper threshold on the oligomer sizes that can be detected by brightness analyses, we shall note that when the dynamics of

the complexes change, then other approaches such as multi-step photobleaching [105] or localization microscopy [106] may be better suited for their study.

Another strength of this protocol is that the steps taken so far to extract the brightness, and hence the oligomerization state of a given GPCR, can be also used for precise *number* determination. Once a brightness value is known it is trivial to extract the number of fluorescent entities by ratio, as illustrated in Figure 4A and Figure 5A. This is of great use for all approaches where it is important to quantify the labeling efficiency of the GPCR of interest, such as GPCRs carrying self-labeling tags, bioorthogonally labeled at the incorporated non-canonical amino acid, or GPCRs targeted by fluorescent ligands. In all these cases, having a robust assay to determine at the single cell level what fraction of the expressed GPCRs carries the label is of great practical use [14]. In our approach, we generate a receptor labeled with a small-molecule fluorophore and a reference C-terminal EGFP (which is mutated at F64L and S65T compared to wtGFP and -whose folding efficiency has been determined to be close to quantitative) (Step1, Option C), or another fluorophore of choice displaying high brightness and rapid maturation time. We screened a few other suitable fluorescent proteins of different colors, based on their reported photophysical properties (Table 2). Figure 8A-B display the number values obtained from temporal and spatial brightness measurements for a Cy3 labeled, TCO*tagged β_2-AR-EGFP. Plotting the number of Cy3 sites vs the EGFP sites (one point = one cell), provides a scatter cloud whose slope corresponds to the labeling efficiency (Cy3/EGFP) (Box 1). We observed this to be a robust and rapid approach to screen a large number of TCO incorporation sites with respect to labeling efficiency, although it may be extended easily to self-labeling tags or fluorescent ligands.

Materials

Biological Materials:

- HEK293AD cells (Biocat, cat. no. AD-100-GVO-CB, RRID:CVCL_KA63) ~~or CHO-K1 (…)~~ Caution: The cell lines used in your research should be regularly checked to ensure they are authentic and are not infected with mycoplasma.

Reagents:

- NEB 5-alpha competent E. coli, high efficiency (New England Biolabs, cat. no. C2987)
- PCR primers for cloning (see Table 3 for the examples used in this protocol)
- Agar microbiology grade (Applichem, cat. no. A0949)
- Effectene Transfection Reagent (Qiagen, cat. no. 301427)
- Lipofectamine 2000 (Thermo Fisher Scientific, cat. no. 11668019)
- Q5 High-Fidelity DNA Polymerase (New England Biolabs, cat. no. M0491)
- Q5 Site-Directed Mutagenesis Kit (New England Biolabs cat. no. E0554S)
- MycoAlert™ Mycoplasma Detection Kit (Lonza, cat. no. LT07-318)
- NEBuilder HiFi DNA Assembly Cloning Kit (New England Biolabs, cat. no. E5520)
- Restriction endonucleases and corresponding buffers of choice (New England Biolabs)
- DNA ligase and corresponding buffer (New England Biolabs, cat. no. M2200S)
- 1kb Plus Ladder (New England Biolabs, cat. no. N3200S)
- DMEM, Dulbecco Modified Eagle's Medium (PAN Biotech cat. no. P04-03500)
- Hank's Buffered Saline Solution (Thermo Fisher Scientific, cat. no. 14025092) Critical: changing the buffer, especially salt composition, may affect the brightness of the fluorophores and adversely affect reproducibility
- FluoroBrite medium (Thermo Fisher Scientific, cat. no. A1896701) Critical: changing the buffer, especially salt composition, may affect the brightness of the fluorophores and adversely affect reproducibility

- Fetal Bovine Serum (Biochrom AG)
- L-Glutamine (PAN-biotech, cat. no. P04-80050)
- Poly-D-Lysine (Fisher Scientific, cat. no. CB-40210)
- DMSO, dimethyl sulfoxide (SigmaAldrich, cat. no. D8418)
- Immersion oil (Leica, cat. no. 13614800) Caution: irritant to skin and eyes
- SNAP-Surface Alexa Fluor 488 (New England Biolabs, cat. no. S9129S)
- SNAP-Cell 505-Star (New England Biolabs, cat. no. S9103S)
- Cy3-H-Tet (Jena Biosceinces, cat. no. CLK-014-05)
- Cy5-H-Tet (Jena Biosceinces, cat. no. CLK-015-05)
- TCO*K (SiChem, cat. no. SC-8008)
- HEPES 1 M, pH 7.4 (Thermo Fisher Scientific, cat. no. 15630106)
- Invitrogen UltraPure Agarose (cat. no. 16500-500), ThermoFisher, Germany
- Modified TAE Buffer (50X) (cat. no. LSKMTAE50), Merck Millipore, Germany

Plasmids

Critical: See Experimental Design – 'Selection of the desired labeling strategy for the GPCR of interest.' for general recommendations regarding construct and protein design. We have used the plasmids below as examples in this protocol. These plasmids can be obtained from the original developers or from the corresponding author of this protocol.

- pcDNA3-SNAP-ADRB2 (New England Biolabs, cat. no. N9184)
- pcDNA3- SigPep-FLAG-SNAP-β_1AR (Calebiro et al. 2013) [51]
- pcDNA3-SNAP-β_2AR (Calebiro et al. 2013) [51]
- pcDNA3-SNAP-CD28
- pcDNA3-β_1AR-EYFP (Dorsch et al., 2009) [81]
- pcDNA3-β_2AR -EYFP (Dorsch et al., 2009) [81]
- pcDNA3-EYFP-β_2AR (Dorsch et al., 2009) [81]
- pcDNA3-CD28-EYFP
- pcDNA3-β_1AR-2xEYFP (Isbilir et al. 2017) [94]
- pcDNA3-SigPep-SNAP-μOR (Möller et al. 2020)[21]
- 98TAG-β_2-AR -EGFP (Serfling et al. 2019)
- pc-SigPep-HA-β_2-AR-EGFP (Serfling et al. 2019) [14]
- 263TAG-CRF$_1$R-EGFP (Serfling et al. 2019) [14]
- MbPylRS^{AF}/4xtRNA^{M15} (Addgene plasmid 105830) [107]

Equipment

- For the steps detailed in this protocol: confocal microscope equipped with at least one photon counting detector (model Leica Confocal Sp8 with 2 HyD detectors and WLL laser). Commerical confocal microscopes (either analog or photon counting) where comparable brightness acquisitions have been successfully employed include (but may not be limited to) Leica SP5, Olympus FV1000,Olympus FV300, Zeiss LSM510/710 (see Table 1).
- PCR Thermocycler (FlexCycler2twin, Analytik Jena)
- Gel running chamber (Biometra Compact M, Analytik Jena, cat. no. 846-025-200)
- T75 flasks (SARSTEDT, cat. no. 50-809-261)
- 6-well plates (SARSTEDT, cat. no.83.3920.300
- Attofluor cell imaging chamber (Thermo Fisher Scientific, cat. no. A7816)
- Round microscope coverslips 25 mm, No. 1.5 (Thermo Fisher Scientific, cat. no. CB00250RAC33MNT0)
- Scalpel or tweezer

Software and Algorithms:

- LASX microscope control software (https://www.leica-microsystems.com/products/microscope-software/p/leica-las-x-ls/)
- GraphPad Prism 7.0 (https://www.graphpad.com/scientific-software/prism/)
- IGOR Pro 7 (https://www.wavemetrics.com/products/igorpro)
- Custom brightness code (as used in Serfling et al., 2019, see code availablility statement)
- ImageJ/Fiji (https://imagej.net/Fiji/ Downloads)
- ImageJ Stowers plugin (https://research.stowers.org/imagejplugins/)
- Microsoft Excel (https://www.microsoft.com/en-us/microsoft-365/excel)

Reagent setup

- **TCO* storage buffer.** Prepare TCO* storage buffer by adding 0.2 M NaOH to a 15% (v/v) DMSO in ultrapure water solution. This buffer is stable at room temperature.
- **TCO*K in TCO* storage buffer.** Prepare a 100mM stock solution of TCO*K in TCO* storage buffer. The TCO*K stock solution can be stored at -80°C for 1 week.
- **HEPES (1 M, pH 7.4).** Stable at 4°C for over a year.
- **Agar plates** were prepared using UltraPure Agarose and Modified TAE buffer and stored up to one month at room temperature
- **HEK293AD cell culture.** Culture HEK293AD cells in Dulbecco's modified Eagle's medium supplemented with 10% (v/v) Fetal Bovine Serum (FBS), 1% L-glutamine, penicillin (100 U/mL), and streptomycin (100 µg/mL) (complete DMEM) or FluoBrite medium supplemented with 10% (v/v) Fetal Bovine Serum (FBS), 1% L-glutamine, penicillin (100 U/mL), and streptomycin (100 µg/mL) (complete FluoBrite). The culture medium can be stored at 4°C for up to one month. Culture cells at 37 °C and 5% CO2 and passage them in T75 flasks every 2-4 days when reaching a confluency of 80-90%. Test cells routinely for mycoplasma contamination using a mycoplasma detection kit.
- **SNAP dye stock solution.** Prepare a 1 mM stock solution of SNAP-Surface 488 dye (or the desired SNAP dye with a different colour) in DMSO. Store the stock solution at -20ºC for up to 3 months.
- **Fluorophore-tetrazine conjugate stock solution.** Dissolve the Fluorophore tetrazine in methanol, split into aliquots of sufficient amounts (e.g. 500 µM) for one experiment and dry the product. Dried aliquots can be stored at -20°C for over a year.
  Prepare a 500 µM fluorophore-tetrazine conjugate stock solution (Cy3-H-tet or Cy5-H-tet) by diluting the dried aliquot in DMSO prior to experiment.

Equipment setup

- Make sure the microscope and laser system have time to warm up before imaging (at least 30 minutes). Switch on the chiller (when present) to keep objective block at constant temperature and minimize thermal drifts and defocus during acquisition. Make sure the microscope sits on a mechanically insulated table. In case of active pneumatic insulation, make sure the system is under pressure and balanced, since mechanical vibration may significantly affect brightness readings.
- The test of the microscope's detectors performance should be performed according to the approach outlined in Box 2 and Extended Data Figure 2: first a dark count statistics needs to be extracted. Then, the brightness of an homogeneous sample (e.g. a dye in a water/glycerol mixture) shall be measured at increasing levels of excitation power to determine if the measured brightness increases proportionally.

Procedure

Generating fluorescent GPCR constructs and controls.

1. We here describe labeling the prototypical β_2-AR using three distinct strategies. Follow Option A for fluorescent protein tagging (EYFP), Option B for self-labeling tags (SNAP) and Option C for labeling using ncAAs. See Table 3 for PCR primers for the examples reported here.

CRITICAL: In this protocol, we use standard plasmid cloning by PCR and restriction enzymes. For detailed cloning guidance, we refer to the following step by step guides from Addgene: https://www.addgene.org/protocols/pcr-cloning/ for CPCR cloning and https://www.addgene.org/protocols/Gibson-assembly/ for Gibson assembly cloning.

(Option A) GPCR fusion to a fluorescent protein Timing: 1 week

I. Amplify by PCR the β_2-AR gene (GenBank: M15169.1) by designing appropriate primers including restriction enzyme cleavage sites (primers **1** and **2** in Table 3).
CRITICAL STEP When performing N-terminal labeling (using primers **5** and **6** in Table 3), make sure to keep the STOP codon in the in the reverse primer (primer **6** in Table 3).
CRITICAL STEP The overlapping sequences of the primers can be used for any GPCR. Only the coding sequence needs to be adapted to the receptor of interest.

II. Digest the target vector and the PCR products from Step I using appropriate restriction enzymes (in this case BamHI and XbaI), purify by agarose gel electrophoresis, and ligate the receptor gene fragment with the vector backbone. We call this intermediate construct pc-β_2-AR –NONSTOP (for C-terminal tagging) or pc-β_2-AR (for N-terminal tagging).
CRITICAL STEP Use a high copy-number vector with an appropriate promoter to mediate high expression levels of the gene of interest. In this protocol we have used pcDNA3 (https://www.addgene.org/vector-database/2092/), which bears a CMV promoter.

III. Subclone the EYFP sequence (GeneBank: AAO48597.1) downstream of the sequence encoding the receptor after PCR amplification with the appropriate primers (primers 3 and 4 in Table 3). Digest the pc-β_2-AR (-NONSTOP) from Step II and the EYFP fragment using **XbaI** and **NotI** and ligate them together.
CRITICAL STEP: For C-terminal cloning of EYFP, make sure that the reverse primer contains an in-frame STOP codon (primer 4 in Table 3). of EYFP (using primers 7 and 8 in Table 3), the reverse primer should not contain a STOP codon (primer 8 in Table 3).
Pause point. Purified plasmid DNA can be stored at -20ºC for months.
?Troubleshooting

IV. Verify cloned constructs by Sanger sequencing using appropriate primers that anneal to at least 18-20 base pairs upstream and downstream regions of the cloned genes.
Pause point. Purified plasmid DNA can be stored at -20ºC for months.
?Troubleshooting

V. Verify the expression and membrane localization of the fluorescently labelled protein in a heterologous expression system using a fluorescence microscope. **See ?Troubleshooting**

CRITICAL As monomeric control, we used the previously published pc-β1-AR –EYFP (available from the authors upon request). As a dimeric control construct, here, we describe the generation of the C terminally 2xEYFP-tagged β1-AR-2xEYFP: Amplify the β1-AR gene (GenBank: NP_000675.1) without a stop codon by PCR using appropriate primers (primers **11** and **12** in Table 3) with restriction enzyme sites.

VI. Digest the amplified PCR product with **HindIII** and **BamHI** and the pcDNA3 vector backbone using appropriate restriction enzymes. Purify the digested DNA, and then ligate the β1-AR fragment into the linearized pcDNA3.

VII. Subclone one EYFP gene without a stop codon to the 3' terminus of the β1-AR gene after PCR amplification using appropriate primers (primers **13** and **14** in Table 3) and subsequent digestion with restriction enzymes **BamHI** and **EcoRI** followed by ligation. We call this intermediate construct pc-β1-AR-EYFP-NONSTOP.

VIII. Prepare the A(EAAAK)4A linker double strand DNA by using synthesized complementary oligonucleotides (primers **15** and **16** in Table 3) with appropriate restriction enzyme sites at 5' and 3' ends. Anneal the complementary oligonucleotides by incubating at 95ºC for 5 minutes and gradually cooling down to 25ºC within 1 hour.

IX. Isolate the annealed oligonucleotide pair by agarose gel electrophoresis and subclone to the 5' of the pc-β1-AR-EYFP-NONSTOP construct by restriction enzyme digestion of the fragment (in this case **EcoRI** and **XbaI**) and the vector backbone, followed by ligation.

X. Subclone a second EYFP sequence with a stop codon to the 3' terminus of the A(EAAAK)4A linker by PCR amplification with the appropriate primers (primers **17** and **18** in Table 3) and appropriate digestion with **XbaI** and **ApaI** followed by ligation. We call this construct β1-AR-2xEYFP.
Pause point. Plasmid DNA can be stored at -20ºC for months after transformation and plasmid DNA isolation. **?Troubleshooting**

XI. Verify the expression and membrane localization of the fluorescently labelled protein in a heterologous expression system using a confocal microscope. **See ?Troubleshooting**

(Option B) GPCR tagging with a SNAP-tag: **Timing: 1 week**

CRITICAL For generating an expression construct with an N-terminally SNAP-tag, we recommend that individual constructs follow this domain structure: pc-SigPep-FLAG-SNAP-GPCR. As an example, we here clone the β_2-AR in this template.

CRITICAL Use pc-SigPep-FLAG-SNAP-β_1-AR (available from the authors upon request) as a template. This construct contains a self-cleavable signaling sequence derived from influenza hemagglutinin, followed by a FLAG-tag, SNAP-tag and the β_1-AR with a stop codon. This construct should also be used as a monomeric control

I. PCR-amplify the β_2-AR with a stop codon by using the appropriate primers with restriction enzyme cleavage sites (primers **19** and **20** in Table 3).
CRITICAL STEP The overlapping sequences of the primers can be used for any GPCR. Only the coding sequence needs to be adapted to the receptor of interest.

II. Digest the pc-SigPep-FLAG-SNAP-β_1AR vector backbone and the PCR-amplified β_1-AR fragment (using NheI and NotI in our example), purify by agarose gel electrophoresis, and then ligate them together. We call this construct pc-SigPep-FLAG-SNAP-β_2-AR.
Pause point. Purified plasmid DNA can be stored at -20ºC for months.

III. Verify cloned constructs by Sanger sequencing using appropriate primers that anneal to at least 18-20 base pairs upstream and downstream regions of the cloned genes.
?Troubleshooting

IV. Verify the expression and membrane localization of the SNAP labelled protein in a heterologous expression system using a fluorescence microscope. **See ?Troubleshooting**

(Option C) GPCR labelling through insertion of non-canonical amino acids Timing: 1.5 weeks

CRITICAL For incorporation of ncAAs into GPCRs and associated analyses (e.g. membrane expression and labeling efficiency), we recommend that individual constructs follow this domain structure: pc-SigPep-HA-GPCR-glycine linker-EGFP. As an example, we here clone the muscarinic M_2 receptor for ncAA incorporation [14].

CRITICAL Use pc-SigPep-HA-β_2-AR -EGFP as a template. This construct contains a self-cleavable signaling sequence derived from influenza hemagglutinin, followed by an HA-tag, the β_2-AR, a TGGGG polyglycine linker and EGFP.

CRITICAL As a monomer control, any biorthogonally tagged GPCR can be used, provided that sub-stoichiometric (sparse) labeling is performed (See Step 2.VIII Option C).

I. Split the template pc-SigPep-HA-β_2-AR -EGFP into two fragments and simultaneously delete the β_2-AR in two PCR reactions (Using primers **21** and **22** from Table 3 for the first reaction, and primers **23** and **24** for the second reaction). The coding sequences of the indicated primers can be used to for generation of any GPCR plasmid. Only the overlapping sequences must be specific to the receptor of interest (as exemplified here with the M2R receptor).

II. PCR out your receptor of interest from its plasmid using the appropriate primers (primers **25** and **26** from Table 3 for our example).
CRITICAL STEP The overlapping sequences of the primers can be used for any GPCR. Only the coding sequence needs to be adapted to the receptor of interest.

III. Generate the desired plasmid (in our example pc-SigPep-HA-M_2R-TGGGG-EGFP) by a 3-fragment assembly of the gel-purified PCR products using the NEBuilder HiFi DNA Assembly Cloning Kit according to the manufacturer's instructions.

IV. For future incorporation of non-canonical amino acids, introduce an amber codon (TAG) at the position of interest using the Q5® Site-Directed Mutagenesis Kit according to the manufacturer's instructions.
Pause point. Purified plasmid DNA can be stored at -20ºC for months.

V. Verify cloned constructs by Sanger sequencing using appropriate primers that anneal to at least 18-20 base pairs upstream and downstream regions of the cloned genes.

Sample preparation and labeling.

2**.** When using GPCR constructs tagged with a fluorescent protein (from Step 1 Option A) or a small self-labeling tag (from Step 1 Option B), prepare the samples as described in Option A. When using constructs that have an amber codon for labeling using non-canonical amino acids (from Step 1 Option C), prepare the samples as described in Option B.

(Option A). Sample preparation for GPCRs labeled with a fluorescent protein or SNAP tag Timing: 2 days.

I. Seed 3x10^5 HEK293AD cells on clean glass 24 mm glass coverslips in 6-well-dishes in a total volume of 2 mL cell culture medium.
CRITICAL STEP Coverslips can be pretreated with poly-D-lysine hydrobromide (MW 500-550 kDa, 25 µg/mL for 30 minutes at room temperature) to improve and accelerate cell adhesion.
CRITICAL STEP For each half-day experimental session prepare at least three coverslips to allow for sufficient replicates. Ideally, data from three such experimental session should be combined.

II. 6-8h after seeding, transfect HEK293AD cells (which by now should be at a 40%-50% confluence with the plasmid carrying the GPCR of interest fused to a fluorescent protein (from Step 1 Option A) or self-labeling tag (from Step 1 Option B) and the appropriate controls. Use Effectene according to the manufacturer's instructions to transfect 0.6 µg DNA/well. Incubate the DNA with enhancer for 5 minutes, and the mixture with the Effectene for at least 15 minutes.

III. 12h after transfection, take the cells from the incubator and gently remove the medium and replace with fresh, pre-warmed, growth medium. When using GPCRs

tagged with fluorescent proteins, proceed directly to Step 3. When using SNAP-tagged, proceed with Steps IV-VIII in this Option.

IV. ***SNAP-tag labeling (Steps IV-VII):*** 24 hours after transfection in Step I, prepare a fresh labeling SNAP-Surface dye working solution by diluting the SNAP dye tock solution 1:1000 (1 µM final concentration) in DMEM. We observed this lower dilution compared to the 1:200 recommended by the manufacturer to work as well [13].
Critical Step. Be sure to vortex well and spin down the SNAP dye stock solution using a table-top centrifuge before pipetting out the solution. Be extra careful when pipetting due to the increased viscosity of the DMSO.

V. Rinse the cells once with 2 mL DMEM, and exchange the medium with 2 mL freshly-prepared labeling medium. Incubate the cells for 30 minutes at 37°C and 5% CO_2.

VI. Wash the cells by incubating for 5 minutes in 2 mL culture medium. Repeat this step twice.

VII. Wash the cells three times with 2 mL DMEM to remove any unbound dye. Remove the DMEM and add 2 mL HBSS buffer to the cells to prepare them for imaging.

VIII. (Optional) Determine the labeling efficiency as described in Box 1.

(Option B) Sample preparation and labeling of ncAAs with tetrazine dyes: Timing: 2 days.

I. Seed $1.8x10^5$ HEK293AD cells on clean glass 24 mm glass coverslips in 6-well-dishes in a total volume of 2 mL cell culture medium.
CRITICAL STEP Coverslips can be pretreated with poly-D-lysine hydrobromide (MW 500-550 kDa, 25 µg/mL for 30 minutes) to improve and accelerate cell adhesion.
CRITICAL STEP For each half-day experimental session prepare at least three coverslips to allow for sufficient replicates. Ideally, data from three such experimental session should be combined.

II. For each 6-well plate, premix 30 µl TCO*K stock solution with 120 µl HEPES (1 M, pH 7.4). Add 25 µl TCO*K solution in HEPES to each well and mix gently. The TCO*K concentration in the medium is 250 µM, a concentration we recommend for extracellular labeling.

III. 1 h after TCO*K loading, co-transfect HEK293AD cells with *Mb*PylRS^{AF}/4xtRNA^{M15} and the receptor construct and the appropriate controls (from Step 1 Option C) in a 1:1 ratio for a total amount of 1.5 µg DNA using Lipofectamine 2000 [107].

IV. 12h after transfection, take the cells from the incubator and gently remove the medium and replace with fresh, pre-warmed, growth medium. …

V. 16-20 h post-transfection transfer the cover glasses to new 6-well plates containing 2 mL dye-free FluoroBrite medium or HBSS.

VI. Incubate cells at least 2h at 37°C under CO_2 (5%) atmosphere.

VII. Dissolve the 500 µM fluorophore-tetrazine conjugate stock solutions (Cy3-H-tet or Cy5-H-tet) in FluoroBrite medium to create two working solutions of 0.15 µM and 1.5 µM. These solutions can then be mixed in the desired ratio for competitive labeling experiments. Prepare 2 mL solution for each well.
CRITICAL STEP: For the monomeric control, create a working solution that contains a 10:90 ratio of the Cy3 and Cy5 labels by combining 0.15 µM Cy3 + 1.35 µM Cy5.

VIII. Apply 2 mL of the solution to the cells for 5 minutes at 37°C. Before imaging, rinse the cells once with 2 mL Fluorobrite medium when performing extracellular labeling. When performing intracellular labelling, incubate the cells for 2 h in 2 mL complete Fluorbrite medium to remove any excess label.

IX. (Optional) Determine the labeling efficiency as described in Box 1.

Data acquisition by confocal microscopy. Timing 6h for temporal brightness, 3h for spatial brightness

3. Start the confocal microscope (here we describe the procedure specific to the SP8 confocal laser scanning microscope using Leica LAS X software). Follow the recommended startup sequence Body and PC, Confocal Head, and Laser.

4. Place coverslips with labeled cells in a stainless cell imaging chamber, such as the Attofluor cell chamber, by carefully lifting the coverslip from the 6 well dish using a scalpel or a tweezer.
   Critical step! If coverslips are removed too harshly, they may crack.
   Critical step! Carefully wipe the bottom glass of the imaging chamber to remove any residual solution, and make sure there are no leaks. We recommend using a piece of tissue paper along the lower rim of the Attofluor chamber to check for leaks. Apply caution when tightening the chamber not to apply too much pressure and break the glass. Glass shards and debris in the lower ring of a not properly cleaned chamber are a common source of asymmetry which leads to cracks in the coverslip.
5. Place the chamber onto the stage of the microscope, after applying the appropriate immersion medium to the front lens of the objective. For a Leica 40x/1.3 NA objective we use immersion oil with a refractive index n_{oil}= 1.518.
6. Enable the white light laser (WLL) and set it to an output of 85% (or equivalently the Argon Ion/diode laser present on the microscope). This is not the final output of the laser after the objective, which can be modulated by using the Acousto Optic Tunable Filter (AOTF) controls in the LAS X software.
   - EYFP: WLL output = 514 nm, detection = 520-600 nm
   - SNAP surface 488: WLL output = 488 nm, detection = 500-550 nm
   - ncAAS with Cy3 tetrazine dye: WLL output = 561 nm, detection 570-650 nm
   - ncAAS with Cy5 tetrazine dye: WLL output 633 nm, detection 650-700 nm

7. Set the AOTF output of the appropriate laser wavelength to low power (0.1%-0.3% in our system) to search for cells without photobleaching them. Set a high scan rate (700 Hz), and a low zoom (1x) to search for transfected/labeled cells. At this point it is important to look that cells appear display a healthy morphology and that those transfected display a correct expression and localization of the construct (See Figure 2 as a reference).
   Caution! Do not search for cells using epifluorescence illumination, such as a Xenon or Mercury lamp, in order to prevent photobleaching. When searching for cells, minimize the excitation dose, or the number and brightness value from the later acquisition will be affected.
   Critical Step! Enable the Hybrid Detectors and use them in photon counting mode. If gating is possible (pulsed laser output from WLL), enable it with a time window between 0.2 ns and 6 ns. This will reduce background due scattering (which by definition has no lifetime).
   Critical step! Keep an eye on the contrast bar next to your imaging window, as it will rescale automatically to the maximum value (256 in case of an 8 bit acquisition mode). Especially if weakly expressing cells are needed, make sure to rescale it to the lower intensity range.
   ?Troubleshooting
8. Identify the lowest expressing cells and the highest expressing cells. Select cells that have an average intensity value in between such two extremes for imaging, and display a homogeneous basolateral membrane.
9. For collecting Temporal Brightness movies, follow Option A. For Spatial Brightness imaging, follow Option B.

Option A: Acquisition of temporal brightness movies

I. Zoom in to the cell of interest. If using a 40x/1.25 NA oil immersion objective, a zoom-factor of 22.8 yields a pixel size of 50 nm in our setup at an image size of 256x256 pixels.
II. Switch on the autofocus (for Leica, Adaptive Focus control) and set an interval of 1 s between each frame of the acquisition to allow sampling different statistical

ensembles at each time point. If no autofocus is available, make sure there is no lateral or axial drift during the acquisition.

III. Set the scanner speed of 400 Hz and the image size to 256x256 pixels, still with the zoom factor of 22.8 (or equivalent, yielding a pixel size of 50 nm, see also Experimental Design). The number of frames and time interval can be inserted in the appropriate *Image Series* panel.
Critical step! Acquire sets of 100 frames (minimum recommended is 50 frames to reach adequate photon count statistics). Identify a laser power which leads to maximal 10% loss of signal (first to last frame) due to photobleaching by recording an image series, using the xyt acquisition mode of the microscope.
?Troubleshooting

IV. Perform partial photobleaching by first zooming out until the entire cell is visible in the field of view and then increasing the laser power to its maximum (100% in the Leica AOD) (switch off the HyD detector/PMT to avoid overload). Photobleach for 10-30 seconds depending on the desired level of photobleaching. Repeat Step 9.III Option A.

V. Image at least 10 cells per condition by repeating steps 9.I-IV Option A, save the experimental workspace by clearly labeling acquisition performed before and after photobleaching.
Critical step! Since oligomerization states might depend on the expression level, we advise to select cells that have a comparable expression range, as determined by the intensity values measured in Step 9.III Option A.

Option B: Acquisition of spatial brightness movies

I. To acquire single images of each cell use a zoom factor to 11.37x (or other appropriate) in order to reach a pixel size of 50 nm.

II. Switch on the autofocus (for Leica, Adaptive Focus control). If no autofocus is available, make sure there is no lateral or axial drift during the acquisition.

III. Set scan rate to 100 Hz. Use 512x512 pixels to maximize area of the field of view and acquire one single frame.

IV. Zoom out until the entire cell is visible in the field of view, increase the laser power to maximum (switch off the HyD detector to avoid overload) and acquire for 10-30 seconds depending on the desired level of photobleaching. Repeat Step 9.III Option B on the bleached sample.

V. Image at least 10 cells per condition by repeating Steps 9.I-9.IV Option B, save the experimental workspace by clearly labeling acquisition performed before and after photobleaching.
Critical step! Since oligomerization states might depend on the expression level, we advise to select cells that have a comparable expression range, as determined by the intensity values measured in Step 9.III Option B.

Data analysis and interpretation. Timing: 1 day

10. Open the experiment.lif file, containing the Temporal or Spatial Brightness image series using ImageJ/Fiji or any other software of choice able to generate as output tiff files. Save the relevant temporal brightness time series or spatial brightness images as multi-page tiff files and simple tiff files respectively, choosing as output format unsigned 16 bits. Make sure that, depending on your operating system, the appropriate 'endianness' is selected. If using ImageJ in windows, check 'Save Tiff' and 'Raw in Intel byte order' under *Edit/Options/Input-Output*.
11. Load the tiff files using IgorPro, using the *Load as Image* command, and checking the option 'Load Multiple Images from File'. Set the count number to -1 to load all pictures. Load and compile the "*brightness protocols.ipf*" procedure file.
12. Analysis of temporal brightness movies (Option A) and spatial brightness images (Option B)

Option A: Analysis of temporal brightness movies

I. Copy the header of the function temporal_brightness() to the command line and run it. This will prompt a popup window where the temporal brightness movie of interest can be selected. If bleaching or slow fluctuations of the sample are present, enable the Boxcar filtering routine (See Experimental Design, Confocal microscopy data acquisition and data analysis).

II. Select a ROI using the polygon tool, as prompted, on the intensity plot. Make sure to select a large ROI which encompasses the whole cell and click *continue*. The average intensity and the brightness figures will pop-up, as shown in (Figure 4). From the *image* menu, select 'modify image appearance' and set as *last color* a value of 2 or 3 (note that 1 represents the baseline brightness value of the background). This will highlight better the different brightness values in the spectral color scale.

?Troubleshooting

III. Compare the brightness image and the intensity image and determine which area of the basolateral membrane to analyze further. Select this area using the *brightness menu*/*highlight on intensity plot.* A new popup window with the image of the cell will appear, allowing a polygonal selection of the region of interest on the basolateral membrane.

Critical step! Once a polygon is selected that excludes the most obvious heterogeneities on the intensity plot and matches a region of homogeneous appearance on the brightness plot, click *continue*. The command line will display the resulting average intensity and brightness from the region (See Experimental Design). A new popup window will also display the histogram of the measured brightness values.

?Troubleshooting

IV. Use the Gaussianity score output on the command line to optimize ROI selection iterating Step 9.III Once an optimal selection has been made, note down the molecular brightness and average intensity from the selected ROI.

Option B: Analysis of spatial brightness images

I. Copy the header of the function SpIDA_photoncounting() to the command line and run it. This will prompt a popup window where the spatial brightness image of interest can be selected.

II. Select a ROI using the polygon tool, as prompted, on the intensity plot. Make sure to select a ROI which avoids visible heterogeneities and encompasses a homogeneous region of the basolateral membrane (See Figure 6). The command line will output the average particles concentration (/PSF) and their brightness.

III. Select the ROI as prompted on the intensity plot. The brightness histogram will pop-up, as shown in Figure 6. Adjust the ROI selection until a maximal Gaussianity score for the intensity values has been obtained. Note down the molecular brightness and average intensity for the selected ROI.

?Troubleshooting

13. The temporal and spatial brightness values should now be compared to the values measured from the control samples. The spatial and temporal brightness values for the sample *x* under investigation can be normalized to the corresponding monomer control brightness (B_M) using the relation ($B_{fold}=B_x-1/(B_M-1)$, yielding the representation displayed in Figure 7B.

14. Collect in an Excel spreadsheet as columns all the brightness values extracted for each individual ROI within each single cell. Do this both for temporal and spatial brightness data and calculate their average and s.e.m. Display the resulting averages in a scatter plot, as illustrated in Figure 7A and Figure 7B (see also Extended Data Figure 3).

?Troubleshooting

(Box 1) Determining the labeling efficiency. Timing: 1 day

CRITICAL: This box describes how to quantify the labelling efficiency when using self-labeling tags, fluorescent ligands or bio-orthogonal labeling. Cells expressing a control receptor carrying a c-terminal EGFP (or another fluorescent tag to be used as a reference [see Table 2]) is required here.

1. Acquire movies in two colors, by following Steps 9.I-9.IV option A of the main procedure using the 'sequential acquisition' mode of the microscope. Acquire multiple movies (10-30) of cells displaying different expression levels, ranging from the lowest to the highest expression levels found in the transiently transfected cells based on their intensity values.
2. In the first sequential step, activate the laser and detector corresponding to the first fluorophore to be imaged. For EGFP in our example of Figure 8, this means switching on a 488 nm line and enabling the first HyD detector in the 500-500 nm range.
3. In the second sequential step, activate laser and detector corresponding to the fluorophore whose labeling efficiency needs to be assessed. In our example of Figure 6 we use Cy3, requiring a 561 nm excitation and detection in the 590-650nm spectral window for HyD2. Use 'sequential by frame' mode, to minimize delay between acquisition. In only one HyD is available, then use a 'by frame' mode.
4. Calculate number and brightness for both channels according to Step 9.I-V Option A of the main procedure.
5. Plot the number data from channel one against the other channel and fit with a line using the software of choice (Extended Data Figure 3 shows an example using ImageJ and Excel), setting the intercept to 0. The slope of the line reports on the labeling efficiency.

   ?Troubleshooting

-END OF BOX 1 -

Timing

Step 1, Generating fluorescent GPCR constructs and controls
- Option A (EYFP cloning) 1 week
- Option B (SNAPtag cloning) 1 week (SNAPtag cloning)
- Option C (ncAA incorporation and mutagenesis) 1.5 weeks

Step 2, Sample preparation and labeling.
- Option A 2 days
- Option B Sample preparation and labeling of ncAAs with tetrazine dyes: 2 days

Steps 3-9, Data acquisition by confocal microscopy. Timing 6h for temporal brightness (Option A), 3h for spatial brightness (Option B)

Steps 10-12, Data analysis and interpretation. 1 day

Box 1, Determining the labeling efficiency. Timing: 1 day

Box 2, Analog detector calibration. Timing: 1 day

Troubleshooting

Troubleshooting guidance can be found in Table 4.

Table 4. Troubleshooting table

Step	Problem	Possible reason	Solution
1	No colonies	One of the many steps of cloning has failed.	For general molecular biology guidance, we refer to the comprehensive resource present on Addgene (https://www.addgene.org/protocols/#plasmidcloni

			ng)
1	GPCR construct is retained in the ER	While the inclusion of a SigPep sequence should circumvent this occurrence, it is possible that the overexpressed construct is retained in the ER. This may relate to the transfection time or even to the transfection method.	Try a longer transfection time (e.g. 48 h). Try a different transfection reagent, e.g. Lipofectamine instead of Effectene. Sometimes, a new construct altogether needs to be designed and tested.
1	Expression level is very low	The promoter is not driving a sufficiently strong expression. There may not be SigPep. The protein may degraded.	Make sure the GPCR is downstream of a strong promoter, such as the CMV promoter in pcDNA3.0/3.1. Screen transfection conditions. When using Effectene, follow the optimization guidelines provided by the manufacturer. be
1	No fluorescent cells can be observed under the confocal microscope	When using photon counting, photon counts are just a few (10-50) in a typical Temporal Brightness acquisition.	Adjust the contrast bar to the average photon counts value. the
2	No labeling can be observed in the SNAP-tag channel	When diluting the dye from the DMSO stock solution, the sample may have been properly mixed	Make sure to vortex and spin down all vials containing dyes before pipetting them. If the stock dye solution is stored under inappropriate conditions, prepare a new stock solution. Make sure that the stock dye solution is stored at -20ºC not maximum for 3 months and protected from light.
2	No or weak labeling can be observed in the Cy3 channel	See the previous entry in this table. It is also possible that the position where the UAG included is favorable labeling. Oftentimes, neighboring amino acids can display	Perform another round of mutagenesis to incorporate the amber stop codon at another position in the protein backbone. Determine the labelling efficiency as described in Box 1. was not for

		drastically different labeling efficiencies [14]	
7	The receptor aggregates/clusters	This may depend on the trafficking behavior of the individual GPCR. If inhomogeneitie s take the form of small clusters, it may be high internalization due to constitutive activity of receptor. may also occur if the expression level of the receptor is too high.	Look for cells displaying a visible lamellipodium, since this is generally a region where membrane expression is more homogeneous. Alternatively, image at the basolateral membrane under the cell nucleus. the This
9	The sample defocuses during image acquisition	There may be residual thermal drift in the microscope.	Make sure an autofocus system is enabled. In the absence of an autofocus system, make sure temperature is stabilized, and that the microscope has been on and running for at least 30 minutes before performing a brightness measurement. Acquire a test image series with the low laser power used for searching cells. Assess the intensity change along the acquired image series. Find a laser power where no photobleaching is observed.
9	The intensity drops during acquisition	This may be due to defocus (see previous entry in table) or to photobleaching .	Make sure the microscope is stabilized and that the laser power used is not photobleaching substantially (e.g. >10% over 100 frames) the this sample.
12	It is difficult to find a homogeneous region on the plasma membrane	For certain receptors, expression pattern may not favor an homogeneous expression pattern. Issues may arise due to interaction of the receptor with intracellular structures actin), its trafficking recycling.	Perform the analysis on smaller polygonal regions. the It is possible to analyze multiple small (2 µm diameter) polygonal ROIs from each cell, and then average their brightness together. This makes it easier to go around widespread inhomogeneity. (e.g. and

12	Brightness is very low, comparable to outside cell .	Low brightness can occur because: receptor is immobile (in TB movie), the laser power is too low or if expression levels are too low: for cells expressing less than 1 receptor /μm^2 the brightness averages the background.	Increase the laser power and repeat the acquisition. If the problem is not solved, it is the possible that expression level is too low. Find a cell expressing higher receptor levels. Cross avalidate your result using spatial brightness. with
12	Brightness is unreasonably high	High brightness can stem from uncorrected fluctuations. A motile cell, or substantial photobleaching can affect be the cause.	Check that the laser power is not photobleaching your fluorophore and that the sample is not drifting. Cross validate your result using spatial brightness.
12	Brightness fluctuates across different experiments	Molecular brightness depends specific instrument conditions. Changes temperature, pinhole alignment detector age can affect it	Prepare and measure often, ideally with each acquisition, also a monomeric reference control for on calibration. in or
14	Temporal and spatial brightness give two different oligomerization behaviors	It is possible that, due to the peculiar trafficking the receptor choice, the two approaches are differentially affected.	Make sure that consistent results are obtained using control constructs, and validate the experimental pipeline using these constructs (such on as the β_1-AR-EYFP and β_1-AR-2xEYFP first). of
14	There is no sizable reduction in brightness upon photobleaching of a construct known to be dimeric	To be effective, photobleaching needs to the entire If only a sub-region of the cell is bleached, unbleached receptors diffuse in, affecting the	We recommend to zoom out (step 16) to encompass the entire cell before performing target photobleaching, and allow sufficient time (1-2 cell minutes) for the system to relax to equilibrium. will

		readout.	
Box 1	A labeling efficiency of over 100% is reported	If one of the two fluorophores is photobleached more than the other, number quantification is affected.	Make sure that while searching for expressing cells (step 10) there is no quantifiable bleaching of EGFP.
		Since EGFP is expressed intracellularly, while labeling (Steps 4 and 5) is extracellular, receptor trafficking may induce apparent higher brightness in this channel, leading to reduced number values	Make sure the ROI selection is appropriate. Make also smaller and check if the recorded brightness decreases. If this is the case, use many -as small as possible- ROIs for the analysis. Validate your results using SB.

Anticipated Results

This first aim of this protocol is to generate a labeled GPCR of interest, together with the necessary sets of controls appropriate to perform a quantitative molecular brightness experiment. For all of the labeling strategies proposed (fluorescent protein tagging, SNAP labeling or bio-orthogonal labeling), the control GPCRs are designed so that they display a monomeric fingerprint in a molecular brightness experiment. The monomeric behavior of the monomeric control GPCR can be appraised by single molecule tracking experiments [13] or photobleaching experiments using brightness itself (Figure 3B-C). When using SNAP-labelling or bio-orthogonal labelling, the receptor of interest can be used as its own monomer control by sparsely labeling the GPCR of interest (Figure 3D). In general, successful experiments and correct brightness outputs can be assessed by monitoring number changes in response to a titration of the labeling dye, since increase the number N of receptors increases with the concentration of the dye, until saturation is reached when all receptors present are labeled.

High quality confocal images of the basolateral membrane of living cells expressing labeled GPCRs shall result into homogeneous regions yielding a steady, although flickering signal. The flickering reflects the out of equilibrium fluctuations of the fluorescently tagged receptors as they diffuse on the plasma membrane (Figure 4B). Proper expression patterns for a set of different GPCRs and labeling approaches are displayed in Figure 2 . Optimization of cell culture, transfection and labelling conditions may be necessary to obtain this quality of basolateral expression and fluorescence signal (See Troubleshooting). Our protocol is optimized to maximize receptor expression at the plasma membrane, but it is still possible that depending on the receptor of choice or the label used, membrane expression may not be satisfactory or homogeneous enough (see Troubleshooting).

Figures 3 and 4 show examples where oligomerization information (that is, measuring a molecular brightness) is collected only from those regions that are in equilibrium and where fluorescence fluctuations arise from the diffusion of the mono/oligomers in and out of the pixels of interest. The Gaussianity score should allow quantifying how good the area

selection was (Figure 6). The Gaussianity test is not biased by the size of the oligomer, but rather by how homogeneous they are. In other words, a region containing homogeneously dispersed decamers will look as gaussian as a region containing homogeneously dispersed monomers.

The oligomerization results for the receptor of choice can be assessed intuitively by plotting the brightness behavior in a 2D graph, as we show in Figure 7A. The control β_1-AR sets the value for the monomer both along the spatial and temporal axes. Bleaching values for the control β_1-AR should fall on the same position in the graph as the unbleached (see Troubleshooting if this is not the case). If a dimeric (or higher oligomerization degree) control is present, such as the β_1-AR-2xEYFP, its brightness εshould be at double the value for the monomer control along both axes. The line passing through these two points defines the monomer-dimer axis along which the oligomerization level of the receptor of choice can be placed. If a protein has a partial oligomeric fingerprint, it will immediately show on this representation, as we see it is the case for the membrane receptor CD86 or the β_2-AR (Figure 7A). Deviations from the monomer-dimer line in the 2D representation do not necessarily represent an aberrant behavior but could also be ascribed to the specific trafficking behavior of the receptor of choice.

A combination of different labeling strategies is also possible, as we show in Figure 7B for the μ-OR, labeled with SNAPtag (or bio-orthogonal labelling) for spatial brightness measurements and EYFP for temporal brightness acquisitions. The protocol can be further adapted to screen for the efficiency of any alternative GPCR labeling strategy. This ability to perform competitive double labelling can be exploited to determine the labelling efficiency of the GPCR of interest, as demonstrated here with a Cy3-labeled, TCO*incorporated β_2-AR-EGFP. By measuring cells with different expression levels and measuring the brightness of the small-molecule dye of interest (Cy3 in our example), its concentration at the plasma membrane can be determined. We used this strategy for screening the labeling efficiency of tree mutations sites in the TCO* incorporated β_2-AR-EGFP. If, for example, temporal brightness is used in the screening, the most promising candidates can then be cross-validated using spatial brightness.

Reporting Summary

Further information on research design is available in the Nature Research Reporting Summary linked to this article.

Data availability

The original data for the experiments shown in Figures 3-8 are available as Source Data with this protocol.

Code availability

The data analysis for this study was done using our custom- made IgorPro™ routine available on GitHub https://github.com/PaoloAnnibale/MolecularBrightness. Image analysis and conversion was performed using ImageJ, freely available at https://imagej.nih.gov/ij/. The ImageJ Stowers brightness plugins are freely at https://research.stowers.org/imagejplugins/.

Competing Interests

The authors declare that they have no competing financial interests.

Acknowledgments

We acknowledge funding by the Deutsche Forschungsgemeinschaft (German Research Foundation, DFG) CRC 1423, project number 421152132, subproject C03 (to PA and MJL); DFG Cluster of Excellence EXC2046 Math+ (to PA and MJL); DFG CRC 1423, project number 421152132, subproject C05 (to IC and AB); The National Institutes of Health (R01-DA038882; to MJL), and the Elite Network Bavaria graduate program “Receptor Dynamics” (to MJL); DFG Grant CO822/2-1 to IC.

Author Contributions

AI, RS, JM, PA performed data collection, data analysis and developed the data acquisition and analysis procedure. AI, AB and UZ developed the cloning procedure. PA, ABS, RS and UZ contributed analysis tools and materials used in the research. PA wrote the manuscript and initiated the research. AB and AI contributed to writing the manuscript. RT, CDF and MS and MJL contributed edits to the manuscript. PA, IC and MJL supervised the primary research. All authors reviewed the manuscript and approved the final article.

Related links

Key references using this protocol:
Serfling et al. ACS chemical biology 14 (6), 1141-1149, 2019. https://doi.org/10.1021/acschembio.8b01115
Annibale et al. Nature Methods 17, 273–275, 2020. https://doi.org/10.1038/s41592-020-0732-0
Möller et al. Nature Chemical Biology 16, 946–954, 2020. https://doi.org/10.1038/s41589-020-0566-1
Isbilir et al. Proceedings of the National Academy of Sciences, accepted
…

Box 2

Analog detector calibration

When a pure photon counting detection is conducted, and k photons are detected on average, with a variance $\sigma 2$ the equations to determine the molecular brightness ε and number of molecules N within the PSF are as follows:

$$\boldsymbol{B = \frac{\sigma^2}{k} = \varepsilon + 1}$$

$$\boldsymbol{N = \frac{k^2}{\sigma^2}}$$

Detector noise affects the accuracy of the estimation of the molecular brightness: for this reason it is generally advisable to work with photon counting detectors, which represent the state of the art and remove much of the extra steps related to detector calibration. When forced to use an analog detector, the distribution of intensity counts becomes (1) shifted to the right (because of the offset of detector dark counts koff), (2) ‘fatter’ (because of the variance of detector noise σ_0 adds to that due to true molecular fluctuations) and (3) stretched (because of amplification gain S) with respect to the photon counts distribution. In the formulas this becomes [67,75]:

$$\boldsymbol{B = \frac{\sigma^2}{k - k_{off}} - \sigma_0^2 = S(\varepsilon + 1)}$$

$$\boldsymbol{N = \frac{(k - koff)^2}{\sigma^2 - \sigma 0^2} = \frac{\varepsilon n + 1}{\varepsilon}}$$

Practically, this mandates to experimentally determine S, σ_0 and k_{off} in order to calculate n and ε. These values can be extracted by recording the frequency distribution of the detector dark counts (i.e. from an acquisition where no sample nor excitation are present, and the room is kept in the dark), as displayed in Extended Data Figure 2D both for a photon counting and and analog detector.
- END OF BOX 2 -

Figure captions

Figure 1 Overview of the procedure. Step 1: The user is guided through the rational design of his/her receptor of interest as well as associated controls. We discuss three options, ranging from extracellular SNAP-tag labeling (amenable for tagging with benzylguanine-conjugated bright organic dyes) [14], tagging with fluorescent proteins and/or non-canonical amino acid labeling of an extracellular loop. **Step 2:** Cells are transfected with the construct of interests and, when necessary, labeled. When labeling with an organic dye, the labeling efficiency can be quantified using the procedure in Box 1. **Steps 3-9:** Data acquisition for the receptor of interest: movies (Option A)/still snapshots (Option B) of specific regions of the basolateral membrane of an intact cell are acquired in order to extract the number and brightness of the diffusing molecules. **Steps 10-12** A careful area selection in the acquired movies/still-shots is required in order to extract number and molecular brightness values from regions in thermodynamic equilibrium, a pre-requisite for the application of the method. A Gaussianity scoring of the distribution of pixel intensities is implemented according to [12]. **Steps 13-14:** Molecular brightness values obtained from spatial and temporal measurements for the same receptor are compared to controls and are plotted one against the other. This 2D representation allows to identify, once the proper controls have been generated and imaged a monomer-dimer-oligomer line. Data points that fall on this line display a varying degree of di-(oligo-)merization.

Figure 2 Labeling Strategies. Confocal microscopy images of the basolateral membrane of HEK293AD cells expressing (A) β_1-AR-EYFP (B) EYFP-β_2-AR (C) Y_2R SNAP-Cell® 505-Star labeled SNAP-β_1-AR (D) Y_2R labeled using TAMRA-labeled Ahx(5-24)NPY at a concentration of 1 μM (E) Cy3 labeled 98TCO* β_2-AR-EGFP, imaged respectively in the EGFP and (F) Cy3 channel. (G) 263TCO-CRF_1R equimolarly labeled with Cy3 and (H) Cy5. Scale bars are 5 μm.

Figure 3 Partial photobleaching experiments in reference constructs. (A) Different diffusion rates and motion affect the brightness measured by temporal brightness. Pictures represent snapshots of simulated movies. Scale bar is 1 μm. (B) Molecular brightness of β_1-AR-EYFP (n=37), β_1-AR-2xEYFP (n=49), and corresponding brightness values after photobleaching (β_1-AR-EYFP bleach (n=37) and β_1-AR-2xEYFP bleach (n=45)). Mean and s.e.m. are shown. Each point is a single cell measurement, and data points from at least 3 independent transfections are combined. (C) Molecular brightness of SNAP-surface labeled SNAP-β_1-AR (n=51), SNAP-SNAP-CD86 (n=53) and corresponding brightness values after photobleaching (SNAP-β_1-AR bleach (n=51) and SNAP-SNAP-CD86 bleach (n=35)). Mean and s.e.m. are shown. Data points originate from at least 3 independent transfections. (D) Plot of the temporal brightness of Cy3, Cy5 and EGFP for an increasing Cy3 to Cy5 ratio used for labeling 263TCO*-CRF_1R-EGFP. Each data point is the average of at least 12 single cell measurements combined from three independent experiments. Adapted from [14]. Error bars represent s.e.m.

Figure 4 Example of a temporal brightness experiment. (A) Concept. In a pixel (black square) excited by the microscope PSF (blue circle), different numbers of fluorescent molecules (green dots) result into different photon counts (solid color). If the measurement is taken at equilibrium, the average intensity of the photon counts and its variance can be

related by simple relationships, which can be used to determine the average number of molecules in the pixel and their individual brightness. (B) Mosaic containing eight representative frames (out of 100) from a temporal brightness acquisition of the basolateral membrane of a cell expressing β_1-AR -EYFP. The bottom-right panel of the mosaic displays the calculated molecular brightness for each pixel in a false color scale (as indicated by sidebar).The white ROIs highlight regions 'out of equilibrium', yielding a high temporal brightness due to spurious high photon count variance, likely to be caused by macroscopic motions of vesicles (solid circles) or cell edges and protrusions (dashed circle). Scale bar is 5 μm. Color scale represents the apparent brightness. (C) Confocal image of a temporal brightness movie of a portion of a cell basolateral membrane expressing 98TCO*β_2-AR-EGFP labeled with Cy3, imaged with excitation 561 nm and detection 590-650 nm. Scale bar is 5 μm. Color scale represents photon counts. (D) The resulting brightness map. The color scale represents the apparent brightness. (E) Brightness vs Intensity scatter plot, where each point represents a pixel of the image. The two clusters, marked as F and G correspond to the white pixels in panels (F) and (G). The corresponding brightness histograms are shown in the right panels. (H) The average intensity image from the temporal brightness movie illustrates an alternative selection mode, based upon choosing a region in the intensity picture. Right, corresponding brightness histogram.

Figure 5. Example of a spatial brightness experiment. A) Concept. In a region of pixels on the basolateral membrane of a cells, thermodynamics dictates that at equilibrium each pixel has a different molecular occupancy number. The corresponding photon counts (solid color) follow a distribution, that for large enough number of molecules follow a super-Poissonian profile, which for above a few molecules per pixel converges to a Gaussian distribution. The variance of this distribution over its mean, provides the apparent molecular brightness. B) Confocal microscopy image of the basolateral membrane of HEK293-AD cells expressing β_1-AR-EYFP, C) β_1-AR-2xEYFP. D) shows cells expressing β_1-AR-2xEYFP upon photobleaching. Scale bar is 10 μm. E) Histograms of the pixel intensities in the selected ROIs in B-D according to the color code. The brightness and number of molecules values are summarized in the table.

Figure 6. Rational ROI selection. (A) Confocal microscopy image of the basolateral membrane of a HEK293AD cell expressing β_1-AR-EYFP. Superposed are two different ROIs encompassing different areas of the membrane. The red ROI is a good ROI since it encompasses a qualitatively homogeneous region of the basolateral membrane. The blue ROI is bad as in include more heterogeneous hotspots. Scale bar is 10 μm. (B) Histogram of the pixel intensities from the two ROIs in A, with the recovered molecular brightness and number values from spatial brightness analysis. The good ROI has a lower molecular brightness (and correspondingly higher number of detected objects), as expected for the β_1-AR. (C) Simulated ROI where monomers and dimers mix to yield a brightness ε^{theory}=10. The ROI contains obvious hot-spots/clusters, which do not belong to the monomer-dimer dynamics and break thermodynamic equilibrium. If the hotspots are included in the brightness analysis, the intensity histogram largely deviates from Gaussianity, (D) as highlighted by the fit and residuals plot. The Gaussianity score, according to a Kolmogorov-Smirnov test, is 0.07 (the expected value for a pure Gaussian experimental distribution is one). The recovered brightness, extracted from the Gaussian fit, exceeds by almost 30% the theoretical brightness. (E) ROI selection which excludes the most obvious hotspots. The histogram recovers Gaussianity and the brightness drops to much closer to the expected value. The Gaussianity score increases to 0.53.

Figure 7 Labeling efficiency and 2D map of GPCRs oligomerization behavior. (A) 2D brightness map of multiple GPCRs or control constructs, highlighting their oligomerization state, on a scatter plot comparing Temporal (x-axis) and Spatial (y-axis) brightness values. Individual points are displayed as average values ± s.e.m. Sample sizes are: β_1-AR -EYFP

n= 45, CD86-EYFP n=7, β_1-AR-2xEYFP n=18, β_2-AR -2xEYFP n=27, β_1-AR -2xEYFP bleach n=31. Data points are the average of *n* single cell measurements and originate from at least 3 independent transfections. (B) Oligomeric state 2D map for the μOR, compared to β_1-AR and the dimeric control CD28. Individual points are displayed as average values ± s.e.m. Sample sizes are: β_1-AR-EYFP n= 46, SNAP- β_1-AR n=10, μOR-EYFP n=54, SNAP-μOR n=18, CD28-EYFP n=28, SNAP-CD28 n=28. Data points originate from at least 3 independent transfections.

Figure 8 Application of our approach to screen the efficiency of bio-orthogonal labeling of the β_2-AR. (A) Three amber stop codon mutants of the β_2-AR -EGFP are transfected into HEK cells followed by intracellular labeling with TCO. The number (N) of fluorescent entities observed in the Cy3 with respect to those seen in the EGFP channel reflects the labeling efficiency of the TCO*K. The labeling efficiency is dependent on the mutation site. Each point represents a single cell measurement, the data shown is combined from three independent transfections. (B) For one mutation site, the experiment is repeated using spatial brightness, displaying compatible results. Each point represents a single cell measurement, combining at least three independent transfections.

Extended Data Figure 1 Use of fluorescent ligands to label receptor of interest. (left) Confocal image of the basolateral membrane of aHEK293-AD cell expressing the Y_2-receptor c-terminally labeled with EYFP and (center) labeled with 1μM TAMRA-Ahx(5-24)NPY followed by washout. (right) Upon displacement with 10μM unlabeled Ahx(5-24)NPY the fluorescent ligand is almost entirely displaced within tens of seconds. Scale bar: 10 μm.

Extended Data Figure 2 Microscope calibration (A) Theoretical ACF for a sample of 10 particles diffusing in 2D through a PSF with a waist of 0.3 um, with a D=0.1 $\mu m^2/s$. The pixel dwell time should allow for an accurate recording of the fluctuations. A general guideline is for the dwell time to be about 10 times smaller than the decay time of the diffusing species. In this case, the decay time is of the order of 300 ms, so any pixel dwell time smaller than 1 ms would be a very safe choice. The characteristic dwell time used in our TB acquisitions (2.4 μs) is way below this value. However, since the associated frame time is of the order of 640 ms on the Leica microscope, we felt this was the best compromise between an acceptable photon collection and a not too slow acquisition time (about over one minute for 100 frames) (B) Apparent Brightness B vs Intensity scatter plot originating from a movie (256x256 pixels, 100 frames) of a homogeneous mixture of Alexa488 imaged in a 90% glycerol/water (w/w) solution, for increasing values of the laser power. (C) Change of brightness (fold change) as a function of the increase in intensity (fold change). As the mean pixel intensity increases (almost linearly with the laser power), the mean brightness scales proportionally. The linear fit (constrained to 0), has a slope of 0.9, indicating that the increase in intensity is matched by a proportional increase in brightness, as expected. (D) Example of dark count histogram for the Leica SP8 HyD photon counting detector and for the analog PMT, the latter superposed to gaussian + exponential fits (black dashed lines) to determine calibration parameters.

Extended Data Figure 3 Example of labeling efficiency quantification (Box 2) (A) Export dual color movies from the Leica LASX software as TIFF multipage files. (B) Run the N + B processing macro. It relies on a set of plugins developed by Jay Unruh at the Stowers Institute for Biomedical Research. The Macro guides the user in a step by step fashion to convert the TIFF images to 16 bits, apply a moving average detrend to remove effects from photobleaching (optional) and calculate the average intensity and brightness value for each pixel of the movie. (C) As a result, the sum intensity image is displayed in parallel to the Brightness vs Intensity plot (highlighted here as B/S vs I/S plot). Note that this plugin allows also for processing images that were collected with an analog detector (in this case, Slope,

zero Variance and Offset need to be adjusted to the properties of the detector of interest. For a photon counting acquisition, leave as indicated here). A cursor selection allows for selecting those pixels belonging to cluster in as B/S vs I/S plot. These pixels are highlighted in red in the intensity image above. The x-avg value provides the average intensity, while the y-avg value provides the average brightness value extracted from the selected pixels. (D) For each cell analyzed these values can be noted down, and then exported in the software of choice (in this case Excel), where the number of emitter for each channel (Cy3 vs EGFP) can be plotted as a scatter, and fit to a line (constrained through the origin, since in the absence of detectable aspecific binding for EGFP=0 we assume Cy3=0) to determine the labeling efficiency

…

Table 3 PCR primers

PCR primers for the example construct described in the procedure			
Construct/step	Procedure/Step	Primers	Restriction enzyme(s)
β_2-AR without stop codon	1/ Path A: I	Primer **1**: Forward: 5'-AAAggatccATGGGGCAACCCGGGAAC-3' Primer **2**: Reverse: 5'-AAAtctagaCAGCAGTGAGTCATTTGTACTACAATTCCT-3',	**BamH I and XbaI**
EYFP C-terminal	1/ Path A: III	Primer **3**: Forward: 5'-AAAtctagaGTGAGCAAGGGCGAGGAG-3' Primer **4**: Reverse: 5'-AAAgcggccgc**TTA**CTTGTACAGCTCGTCCATGC-3'	**XbaI and NotI**
β_2-AR with stop codon	1/ Path A: IV	Primer **5**: Forward: 5'-AAAgaattcATGGGGCAACCCGGGAAC-3' Primer **6**: Reverse: 5'-AAActcgag**TTA**CAGCAGTGAGTCATTTGTACTACAATT-3'	**EcoRI and XhoI**
EYFP N-terminal	1/ Option A: V	Primer **7**: Forward: 5'-AAAggatccATGGTGAGCAAGGGCGAGGAG-3' Primer **8**: Reverse: 5'-AAAgaattcGAGCCGTACCTGCTCGACATGTTC-3'	**BamH I and EcoRI**
SigPep-FLAG	1/ Option A: VII	Primer **9**: Forward: 5'-CTTaagcttATGAAGACGATCATCGCCCTGAGCTACATCTTCTGCCTGGTgTTCGCCGACTACAAGGACGATGATGACGCCggatccAAA-3' Primer **10**: Reverse: 5'-TTTggatccGGCGTCATCATCGTCCTTGTAGTCGGCGAAcACCAGGCAGAAGATGTAGCTCAGGGCGATGATCGTCTTCATaagcttAAG-3'	**XbaI and ApaI**
β_1-AR	1/ Option A	Primer **11**: Forward: 5'-AATAATAAGCTTATGGGCGCGGGGGTGCTC-3' Primer **12**: Reverse: 5'- AATAATGGATCCCACCTTGGATTCCGAGGCGAA-3'	**HindIII and BamH I,**
β_1-AR 2xEYFP: EYFP1	1/ Option A	Primer **13**: Forward: 5'-AATAATGGATCCGTGAGCAAGGGCGAGGAG-3' Primer **14**: Reverse: 5'- AATAATGAATTCCTTGTACAGCTCGTCCATGCC-3'	**BamH I and EcoRI**
β_1-AR-2xEYFP:	1/ Option A	Primer **15**: Forward: 5'P-aattcGCAGAGGCCGCGGCTAAGGAGGCCGCTGCGAAAGAAGCTGCAGCGAA	**EcoRI and XbaI.**

Rigid Linker		GGAAGCTGCAGCGAAGt-3' Primer **16**: Reverse: 5'P-ctagaCTTCGCTGCAGCTTCCTTCGCTGCAGCTTCTTTCGCAGCGGCCTCCTTAGCCGCGGCCTCTGCg-3'	
β_1-AR-2xEYFP: EYFP2	1/ Option A	Primer **17**: Forward: 5'-AATAATTCTAGAGTGAGCAAGGGCGAGGAGCTG-3' Primer **18**: Reverse: 5'-AATAATGGGCCCTTACTTGTACAGCTCGTCCATGCC-3'	**XbaI and ApaI**
β_2-AR with STOP codon (for SNAP-tag incorporation)	1/ Option B: I	Primer **19**: Forward: 5'-AAAgctagcATGGGGCAACCCGGGAAC-3' Primer **20**: Reverse: 5'-AAAgcggccgc**TTA**CAGCAGTGAGTCATTTGTACTACAATT-3'	**NheI and NotI,**
M_2R-EGFP	1/Option C	Primer **21** (upper-case: priming sequence, lower-case: overlapping N-terminal sequence of the M_2R receptor): 5'-agaggagtttgttgagttattcatGCCAGCGTAATCTGGAACATCGTA-3' Primer **22**: 5'-ATTCTAGTTGTGGTTTGTCCAAACTCATCAA-3'. Primer **23:** (lower-case: overlapping C-terminal sequence of the M_2R receptor without stop codon): 5'-aagaacataggcgctacaaggACCGGTGGCGGAGGCGTG-3' Primer **24**: 5'-TTGATGAGTTTGGACAAACCACAACTAGAAT-3'. Primer **25:** (upper-case priming sequence N-terminus M_2R receptor; lower-case: overlapping sequence HA-tag): 5'-tacgatgttccagattacgctggcATGAATAACTCAACAAACTCCTCTAACAATAG-3' and Primer **26** (upper-case priming sequence C-terminus M_2R receptor without stop codon; lower-case: overlapping sequence glycine linker and EGFP): 5'-cttgctcacgcctccgccaccggtCCTTGTAGCGCCTATGTTCTT-3'.	

Table 2 Recommended fluorescent proteins for quantification of labeling efficiencies. All of the fluorescent proteins reported in this table contain mutations that significantly improve folding and maturation times in comparison to their 'parental' proteins [108]. In particular, the cyan [109] mCerulean and mTurquoise2 [110], as well as the yellow mEYFP [111] and mVenus [112] fluorescent proteins are characterized by F64L, M153T, V163A, and S175G mutations. In addition, yellow proteins contain the F46L mutation, and mEYFP an additional S72A mutation. In the green spectrum, mClover3 [113] and mNeonGreen [114], the mutations F64L, S65T, M153T, V163A significantly improve folding efficiency and maturation times. For the red fluorescent proteins mCherry2 [115] and mScarlet-I [116], the mutations Q66M, M182K are important for efficient folding and fast maturation. Importantly, all of the recommended proteins are reported to be largely monomeric.

Protein name	**Excitation maximum (nm)**	**Emission maximum (nm)**	**Extinction coefficient ($mM^{-1}cm^{-1}$)**	**Maturation time $t_{0.9}$ (min)**
Cyan				
mCerulean	434	475	16	24.0
mTurquoise2	434	474	30	95.1
Green				
mClover3	506	518	85	112.4
mNeonGreen	506	517	93	36.8
Yellow				
mEYFP	515	528	49	30.9
mVenus	515	527	67	18.4
Red				
mCherry2	589	610	18	51.3
mScarlet-I	569	593	56	66.3

Table 1: Key molecular brightness methods and their area of application

Authors	Methods name (acronym)	Key feature	Area of applicability (strength)	Potential pitfalls	Detection Setup
Chen et al.[15]	PCH High temporal resolution and statistics provides brightness from one PSF		Any diffusing protein in a homogeneous environment.	Sensitive to slow fluctuations due to spatial heterogeneity	Custom 2-photon microscope with photon counting detection
Herrick-Davis et al.[64,117]	PCH Proteins diffusing in the apical membrane			Sensitive to slow fluctuations due to membrane movements-receptor trafficking	Zeiss LSM 510 with Confocor unit
Digman et al. [62]	N&B Confocal-Image based. One brightness value per pixel from a time series.		Cytosolic, nuclear and membrane proteins	Acquisition runs of over a minute expose to drift	Olympus Fluoview 1000
Unruh et al. [67]	N&B As above, using widefield CCD camera		Cytosolic, nuclear and membrane proteins	Requires calibration of analog detector	TIRF with Photometrics Cascade EM-CCD camera
Godin et al. [60]	SpIDA Confocal image based: one brightness value from a ROI		Membrane proteins	Hard to discriminate small intensity hot-spots and heterogeneities	Olympus FV400
Cutrale et al. [27]	eN&B EMCCD-image based. One brightness value per pixel from a time series.		Cytosolic, nuclear and membrane proteins. Statistical weighting of coexisting species within each pixel.	Potential limitations for faster species due to exposure time of the camera.	TIRF with Andor EM-CCD camera
Stoneman et al. [118]	FIF Confocal image based: many brightness values from many small ROIs		Membrane proteins, including GPCRs in polarized or spatially heterogeneous systems	Requires spatial segregation of oligomeric species.	Zeiss LSM 510 with photomultiplier tube

References

1 Sachs, J. N. & Engelman, D. M. Introduction to the membrane protein reviews: the interplay of structure, dynamics, and environment in membrane protein function. *Annu Rev Biochem* **75**, 707-712, doi:10.1146/annurev.biochem.75.110105.142336 (2006).

2 Jacobson, K., Sheets, E. D. & Simson, R. Revisiting the fluid mosaic model of membranes. *Science* **268**, 1441-1442, doi:10.1126/science.7770769 (1995).

3 Klingenberg, M. Membrane protein oligomeric structure and transport function. *Nature* **290**, 449-454, doi:10.1038/290449a0 (1981).

4 Matthews, J. M. & Sunde, M. Dimers, oligomers, everywhere. *Adv Exp Med Biol* **747**, 1-18, doi:10.1007/978-1-4614-3229-6_1 (2012).

5 Weis, W. I. & Kobilka, B. K. The Molecular Basis of G Protein-Coupled Receptor Activation. *Annu Rev Biochem* **87**, 897-919, doi:10.1146/annurev-biochem-060614-033910 (2018).

6 Hauser, A. S., Attwood, M. M., Rask-Andersen, M., Schioth, H. B. & Gloriam, D. E. Trends in GPCR drug discovery: new agents, targets and indications. *Nat Rev Drug Discov* **16**, 829-842, doi:10.1038/nrd.2017.178 (2017).

7 Fredriksson, R., Lagerstrom, M. C., Lundin, L. G. & Schioth, H. B. The G-protein-coupled receptors in the human genome form five main families. Phylogenetic analysis, paralogon groups, and fingerprints. *Mol Pharmacol* **63**, 1256-1272, doi:10.1124/mol.63.6.1256 (2003).

8 Pin, J. P. & Bettler, B. Organization and functions of mGlu and GABA(B) receptor complexes. *Nature* **540**, 60-68, doi:10.1038/nature20566 (2016).

9 Whorton, M. R. *et al.* A monomeric G protein-coupled receptor isolated in a high-density lipoprotein particle efficiently activates its G protein. *Proceedings of the National Academy of Sciences of the United States of America* **104**, 7682-7687, doi:10.1073/pnas.0611448104 (2007).

10 Ferre, S. *et al.* G Protein-Coupled Receptor Oligomerization Revisited: Functional and Pharmacological Perspectives. *Pharmacol Rev* **66**, 413-434, doi:10.1124/pr.113.008052 (2014).

11 Hanyaloglu, A. C. & von Zastrow, M. Regulation of GPCRs by endocytic membrane trafficking and its potential implications. *Annu Rev Pharmacol Toxicol* **48**, 537-568, doi:10.1146/annurev.pharmtox.48.113006.094830 (2008).

12 Annibale, P. & Lohse, M. J. Spatial heterogeneity in molecular brightness. *Nature methods* **17**, 273-275, doi:10.1038/s41592-020-0732-0 (2020).

13 Möller, J. *et al.* Single-molecule analysis reveals agonist-specific dimer formation of μ-opioid receptors. *Nat Chem Biol*, doi:10.1038/s41589-020-0566-1 (2020).

14 Serfling, R. *et al.* Quantitative Single-Residue Bioorthogonal Labeling of G Protein-Coupled Receptors in Live Cells. *ACSChem Biol* **14**, 1141-1149, doi:10.1021/acschembio.8b01115 (2019).

15 Chen, Y., Muller, J. D., So, P. T. C. & Gratton, E. The photon counting histogram in fluorescence fluctuation spectroscopy. *Biophys J* **77**, 553-567, doi:Doi 10.1016/S0006-3495(99)76912-2 (1999).

16 Qian, H. & Elson, E. L. Distribution of molecular aggregation by analysis of fluctuation moments. *Proceedings of the National Academy of Sciences of the United States of America* **87**, 5479-5483, doi:10.1073/pnas.87.14.5479 (1990).
17 Isbilir, A. *et al.* Advanced fluorescence microscopy reveals disruption of dynamic CXCR4 dimerization by subpocket-specific inverse agonists. *Proceedings of the National Academy of Sciences of the United States of America* **in press** (2020).
18 Angers, S. *et al.* Detection of beta(2)-adrenergic receptor dimerization in living cells using bioluminescence resonance energy transfer (BRET). *Proceedings of the National Academy of Sciences of the United States of America* **97**, 3684-3689, doi:Doi 10.1073/Pnas.060590697 (2000).
19 Lan, T. H. *et al.* BRET evidence that beta(2) adrenergic receptors do not oligomerize in cells. *Sci Rep-Uk* **5**, doi:Artn 10166
10.1038/Srep10166 (2015).
20 Johnson, J. A., Lu, Y. Y., Van Deventer, J. A. & Tirrell, D. A. Residue-specific incorporation of non-canonical amino acids into proteins: recent developments and applications. *Curr Opin Chem Biol* **14**, 774-780, doi:10.1016/j.cbpa.2010.09.013 (2010).
21 Moller, J. *et al.* Single-molecule analysis reveals agonist-specific dimer formation of micro-opioid receptors. *Nat Chem Biol*, doi:10.1038/s41589-020-0566-1 (2020).
22 Tarasova, N. I. *et al.* Visualization of G protein-coupled receptor trafficking with the aid of the green fluorescent protein. Endocytosis and recycling of cholecystokinin receptor type A. *JBiol Chem* **272**, 14817-14824, doi:10.1074/jbc.272.23.14817 (1997).
23 Barak, L. S. *et al.* Internal trafficking and surface mobility of a functionally intact beta2-adrenergic receptor-green fluorescent protein conjugate. *Mol Pharmacol* **51**, 177-184, doi:10.1124/mol.51.2.177 (1997).
24 Chalfie, M. GFP: Lighting up life. *Proceedings of the National Academy of Sciences of the United States of America* **106**, 10073-10080, doi:10.1073/pnas.0904061106 (2009).
25 Keppler, A. *et al.* A general method for the covalent labeling of fusion proteins with small molecules in vivo. *Nat Biotechnol* **21**, 86-89, doi:10.1038/nbt765 (2003).
26 Liu, C. C. & Schultz, P. G. Adding new chemistries to the genetic code. *Annu Rev Biochem* **79**, 413-444, doi:10.1146/annurev.biochem.052308.105824 (2010).
27 Cutrale, F. *et al.* Using enhanced number and brightness to measure protein oligomerization dynamics in live cells. *Nat Protoc* **14**, 616-638, doi:10.1038/s41596-018-0111-9 (2019).
28 Wallin, E. & von Heijne, G. Genome-wide analysis of integral membrane proteins from eubacterial, archaean, and eukaryotic organisms. *Protein Sci* **7**, 1029-1038, doi:10.1002/pro.5560070420 (1998).
29 Goldstein, B. & Perelson, A. S. Equilibrium theory for the clustering of bivalent cell surface receptors by trivalent ligands. Application to histamine release from basophils. *Biophys J* **45**, 1109-1123, doi:10.1016/S0006-3495(84)84259-9 (1984).
30 Varma, R. & Mayor, S. GPI-anchored proteins are organized in submicron domains at the cell surface. *Nature* **394**, 798-801, doi:10.1038/29563 (1998).
31 Hofman, E. G. *et al.* Ligand-induced EGF receptor oligomerization is kinase-dependent and enhances internalization. *JBiol Chem* **285**, 39481-39489, doi:10.1074/jbc.M110.164731 (2010).

32 Serebryannyy, L. A. *et al.* Persistent nuclear actin filaments inhibit transcription by RNA polymerase II. *JCell Sci* **129**, 3412-3425, doi:10.1242/jcs.195867 (2016).
33 Bock, A. *et al.* Optical Mapping of cAMP Signaling at the Nanometer Scale. *Cell*, doi:10.1016/j.cell.2020.07.035 (2020).
34 Hebert, T. E. & Bouvier, M. Structural and functional aspects of G protein-coupled receptor oligomerization. *Biochem Cell Biol* **76**, 1-11, doi:10.1139/bcb-76-1-1 (1998).
35 Maggio, R., Vogel, Z. & Wess, J. Coexpression studies with mutant muscarinic/adrenergic receptors provide evidence for intermolecular "cross-talk" between G-protein-linked receptors. *Proceedings of the National Academy of Sciences of the United States of America* **90**, 3103-3107, doi:10.1073/pnas.90.7.3103 (1993).
36 Kobayashi, H., Picard, L. P., Schonegge, A. M. & Bouvier, M. Bioluminescence resonance energy transfer-based imaging of protein-protein interactions in living cells. *Nat Protoc* **14**, 1084-1107, doi:10.1038/s41596-019-0129-7 (2019).
37 Mercier, J. F., Salahpour, A., Angers, S., Breit, A. & Bouvier, M. Quantitative assessment of beta 1- and beta 2-adrenergic receptor homo- and heterodimerization by bioluminescence resonance energy transfer. *JBiol Chem* **277**, 44925-44931, doi:10.1074/jbc.M205767200 (2002).
38 James, J. R., Oliveira, M. I., Carmo, A. M., Iaboni, A. & Davis, S. J. A rigorous experimental framework for detecting protein oligomerization using bioluminescence resonance energy transfer. *Nature methods* **3**, 1001-1006, doi:10.1038/nmeth978 (2006).
39 Lohse, M. J. G protein-coupled receptors: too many dimers? *Nature methods* **3**, 972-973, doi:10.1038/nmeth1206-972 (2006).
40 Vilardaga, J. P., Bunemann, M., Krasel, C., Castro, M. & Lohse, M. J. Measurement of the millisecond activation switch of G protein-coupled receptors in living cells. *Nat Biotechnol* **21**, 807-812, doi:10.1038/nbt838 (2003).
41 Nikolaev, V. O., Bunemann, M., Hein, L., Hannawacker, A. & Lohse, M. J. Novel single chain cAMP sensors for receptor-induced signal propagation. *JBiol Chem* **279**, 37215-37218, doi:10.1074/jbc.C400302200 (2004).
42 Benredjem, B. *et al.* Exploring use of unsupervised clustering to associate signaling profiles of GPCR ligands to clinical response. *Nat Commun* **10**, 4075, doi:10.1038/s41467-019-11875-6 (2019).
43 Kauk, M. & Hoffmann, C. Intramolecular and Intermolecular FRET Sensors for GPCRs - Monitoring Conformational Changes and Beyond. *Trends in pharmacological sciences* **39**, 123-135, doi:10.1016/j.tips.2017.10.011 (2018).
44 Pisterzi, L. F. *et al.* Oligomeric size of the m2 muscarinic receptor in live cells as determined by quantitative fluorescence resonance energy transfer. *JBiol Chem* **285**, 16723-16738, doi:10.1074/jbc.M109.069443 (2010).
45 Fish, K. N. Total internal reflection fluorescence (TIRF) microscopy. *Curr Protoc Cytom* **Chapter 12**, Unit12 18, doi:10.1002/0471142956.cy1218s50 (2009).
46 Jonkman, J., Brown, C. M., Wright, G. D., Anderson, K. I. & North, A. J. Tutorial: guidance for quantitative confocal microscopy. *Nat Protoc* **15**, 1585-1611, doi:10.1038/s41596-020-0313-9 (2020).
47 Felce, J. H. *et al.* Receptor Quaternary Organization Explains G Protein-Coupled Receptor Family Structure. *Cell Rep* **20**, 2654-2665, doi:10.1016/j.celrep.2017.08.072 (2017).

48 Moerner, W. E. & Fromm, D. P. Methods of single-molecule fluorescence spectroscopy and microscopy. *Review of Scientific Instruments* **74**, 3597-3619, doi:10.1063/1.1589587 (2003).
49 Scarselli, M. *et al.* Revealing G-protein-coupled receptor oligomerization at the single-molecule level through a nanoscopic lens: methods, dynamics and biological function. *Febs J* **283**, 1197-1217, doi:10.1111/febs.13577 (2016).
50 Wang, X. *et al.* Single-molecule fluorescence imaging to quantify membrane protein dynamics and oligomerization in living plant cells. *Nat Protoc* **10**, 2054-2063, doi:10.1038/nprot.2015.132 (2015).
51 Calebiro, D. *et al.* Single-molecule analysis of fluorescently labeled G-protein-coupled receptors reveals complexes with distinct dynamics and organization. *Proceedings of the National Academy of Sciences of the United States of America* **110**, 743-748, doi:10.1073/pnas.1205798110 (2013).
52 Sungkaworn, T. *et al.* Single-molecule imaging reveals receptor-G protein interactions at cell surface hot spots. *Nature* **550**, 543-+, doi:10.1038/nature24264 (2017).
53 Puthenveedu, M. A. & von Zastrow, M. Cargo regulates clathrin-coated pit dynamics. *Cell* **127**, 113-124, doi:10.1016/j.cell.2006.08.035 (2006).
54 Hern, J. A. *et al.* Formation and dissociation of M-1 muscarinic receptor dimers seen by total internal reflection fluorescence imaging of single molecules. *Proceedings of the National Academy of Sciences of the United States of America* **107**, 2693-2698, doi:10.1073/pnas.0907915107 (2010).
55 Kasai, R. S. *et al.* Full characterization of GPCR monomer-dimer dynamic equilibrium by single molecule imaging. *JCell Biol* **192**, 463-480, doi:10.1083/jcb.201009128 (2011).
56 Giannone, G. *et al.* Dynamic superresolution imaging of endogenous proteins on living cells at ultra-high density. *Biophys J* **99**, 1303-1310, doi:10.1016/j.bpj.2010.06.005 (2010).
57 Post, S. R., Hilal-Dandan, R., Urasawa, K., Brunton, L. L. & Insel, P. A. Quantification of signalling components and amplification in the beta-adrenergic-receptor-adenylate cyclase pathway in isolated adult rat ventricular myocytes. *Biochem J* **311 (Pt 1)**, 75-80, doi:10.1042/bj3110075 (1995).
58 Hesselgesser, J. *et al.* Identification and characterization of the CXCR4 chemokine receptor in human T cell lines: ligand binding, biological activity, and HIV-1 infectivity. *JImmunol* **160**, 877-883 (1998).
59 Hellriegel, C., Caiolfa, V. R., Corti, V., Sidenius, N. & Zamai, M. Number and brightness image analysis reveals ATF-induced dimerization kinetics of uPAR in the cell membrane. *FASEB journal : official publication of the Federation of American Societies for Experimental Biology* **25**, 2883-2897, doi:10.1096/fj.11-181537 (2011).
60 Godin, A. G. *et al.* Revealing protein oligomerization and densities in situ using spatial intensity distribution analysis. *Proceedings of the National Academy of Sciences of the United States of America* **108**, 7010-7015, doi:10.1073/pnas.1018658108 (2011).
61 Ward, R. J., Pediani, J. D., Godin, A. G. & Milligan, G. Regulation of Oligomeric Organization of the Serotonin 5-Hydroxytryptamine 2C (5-HT2C) Receptor Observed by Spatial Intensity Distribution Analysis. *JBiol Chem* **290**, 12844-12857, doi:10.1074/jbc.M115.644724 (2015).

62 Digman, M. A., Dalal, R., Horwitz, A. F. & Gratton, E. Mapping the number of molecules and brightness in the laser scanning microscope. *Biophys J* **94**, 2320-2332, doi:10.1529/biophysj.107.114645 (2008).
63 Hinde, E. *et al.* Quantifying the dynamics of the oligomeric transcription factor STAT3 by pair correlation of molecular brightness. *Nat Commun* **7**, 11047, doi:10.1038/ncomms11047 (2016).
64 Herrick-Davis, K., Grinde, E., Cowan, A. & Mazurkiewicz, J. E. Fluorescence Correlation Spectroscopy Analysis of Serotonin, Adrenergic, Muscarinic, and Dopamine Receptor Dimerization: The Oligomer Number Puzzle. *Mol Pharmacol* **84**, 630-642, doi:10.1124/mol.113.087072 (2013).
65 Parmar, V. K., Grinde, E., Mazurkiewicz, J. E. & Herrick-Davis, K. Beta2-adrenergic receptor homodimers: Role of transmembrane domain 1 and helix 8 in dimerization and cell surface expression. *Biochim Biophys Acta*, doi:10.1016/j.bbamem.2016.12.007 (2016).
66 Hink, M. A., Shah, K., Russinova, E., de Vries, S. C. & Visser, A. J. Fluorescence fluctuation analysis of Arabidopsis thaliana somatic embryogenesis receptor-like kinase and brassinosteroid insensitive 1 receptor oligomerization. *Biophys J* **94**, 1052-1062, doi:10.1529/biophysj.107.112003 (2008).
67 Unruh, J. R. & Gratton, E. Analysis of molecular concentration and brightness from fluorescence fluctuation data with an electron multiplied CCD camera. *Biophys J* **95**, 5385-5398, doi:10.1529/biophysj.108.130310 (2008).
68 Nagy, P., Claus, J., Jovin, T. M. & Arndt-Jovin, D. J. Distribution of resting and ligand-bound ErbB1 and ErbB2 receptor tyrosine kinases in living cells using number and brightness analysis. *Proceedings of the National Academy of Sciences of the United States of America* **107**, 16524-16529, doi:10.1073/pnas.1002642107 (2010).
69 Zamai, M. *et al.* Number and brightness analysis reveals that NCAM and FGF2 elicit different assembly and dynamics of FGFR1 in live cells. *JCell Sci* **132**, doi:10.1242/jcs.220624 (2019).
70 Puthenveedu, M. A. & von Zastrow, M. Cargo regulates clathrin-coated pit dynamics. *Cell* **127**, 113-124, doi:10.1016/j.cell.2006.08.035 (2006).
71 Eichel, K., Jullie, D. & von Zastrow, M. beta-Arrestin drives MAP kinase signalling from clathrin-coated structures after GPCR dissociation. *Nat Cell Biol* **18**, 303-+, doi:10.1038/ncb3307 (2016).
72 Pediani, J. D., Ward, R. J., Godin, A. G., Marsango, S. & Milligan, G. Dynamic Regulation of Quaternary Organization of the M-1 Muscarinic Receptor by Subtype-selective Antagonist Drugs. *JBiol Chem* **291**, 13132-13146, doi:10.1074/jbc.M115.712562 (2016).
73 Golebiewska, U., Johnston, J. M., Devi, L., Filizola, M. & Scarlata, S. Differential response to morphine of the oligomeric state of mu-opioid in the presence of delta-opioid receptors. *Biochemistry* **50**, 2829-2837, doi:10.1021/bi101701x (2011).
74 Dunsing, V. *et al.* Optimal fluorescent protein tags for quantifying protein oligomerization in living cells. *Scientific reports* **8**, 10634, doi:10.1038/s41598-018-28858-0 (2018).
75 Dalal, R. B., Digman, M. A., Horwitz, A. F., Vetri, V. & Gratton, E. Determination of particle number and brightness using a laser scanning confocal microscope operating in the analog mode. *Microscopy research and technique* **71**, 69-81, doi:10.1002/jemt.20526 (2008).

76 Kobilka, B. K. G protein coupled receptor structure and activation. *Bba-Biomembranes* **1768**, 794-807, doi:10.1016/j.bbamem.2006.10.021 (2007).
77 Bohme, I. & Beck-Sickinger, A. G. Illuminating the life of GPCRs. *Cell Commun Signal* **7**, 16, doi:10.1186/1478-811X-7-16 (2009).
78 Daly, C. J. & McGrath, J. C. Fluorescent ligands, antibodies, and proteins for the study of receptors. *Pharmacol Ther* **100**, 101-118, doi:10.1016/j.pharmthera.2003.08.001 (2003).
79 Lohse, M. J., Nuber, S. & Hoffmann, C. Fluorescence/bioluminescence resonance energy transfer techniques to study G-protein-coupled receptor activation and signaling. *Pharmacol Rev* **64**, 299-336, doi:10.1124/pr.110.004309 (2012).
80 Naganathan, S., Ye, S., Sakmar, T. P. & Huber, T. Site-specific epitope tagging of G protein-coupled receptors by bioorthogonal modification of a genetically encoded unnatural amino acid. *Biochemistry* **52**, 1028-1036, doi:10.1021/bi301292h (2013).
81 Dorsch, S., Klotz, K. N., Engelhardt, S., Lohse, M. J. & Bunemann, M. Analysis of receptor oligomerization by FRAP microscopy. *Nature methods* **6**, 225-230, doi:10.1038/nmeth.1304 (2009).
82 Emami-Nemini, A. *et al.* Time-resolved fluorescence ligand binding for G protein-coupled receptors. *Nat Protoc* **8**, 1307-1320, doi:10.1038/nprot.2013.073 (2013).
83 Hoffmann, C. *et al.* A FlAsH-based FRET approach to determine G protein-coupled receptor activation in living cells. *Nature methods* **2**, 171-176, doi:10.1038/nmeth742 (2005).
84 Kuder, K. & Kiec-Kononowicz, K. Fluorescent GPCR ligands as new tools in pharmacology. *Curr Med Chem* **15**, 2132-2143, doi:10.2174/092986708785747599 (2008).
85 Magalhaes, A. C., Dunn, H. & Ferguson, S. S. Regulation of GPCR activity, trafficking and localization by GPCR-interacting proteins. *Br JPharmacol* **165**, 1717-1736, doi:10.1111/j.1476-5381.2011.01552.x (2012).
86 Al-Sabah, S., Adi, L., Bunemann, M. & Krasel, C. The Effect of Cell Surface Expression and Linker Sequence on the Recruitment of Arrestin to the GIP Receptor. *Front Pharmacol* **11**, 1271, doi:10.3389/fphar.2020.01271 (2020).
87 Schoneberg, T. *et al.* Mutant G-protein-coupled receptors as a cause of human diseases. *Pharmacol Ther* **104**, 173-206, doi:10.1016/j.pharmthera.2004.08.008 (2004).
88 Guan, X. M., Kobilka, T. S. & Kobilka, B. K. Enhancement of membrane insertion and function in a type IIIb membrane protein following introduction of a cleavable signal peptide. *JBiol Chem* **267**, 21995-21998 (1992).
89 Gautier, A. *et al.* An engineered protein tag for multiprotein labeling in living cells. *Chem Biol* **15**, 128-136, doi:10.1016/j.chembiol.2008.01.007 (2008).
90 Los, G. V. *et al.* HaloTag: a novel protein labeling technology for cell imaging and protein analysis. *ACSChem Biol* **3**, 373-382, doi:10.1021/cb800025k (2008).
91 Maurel, D. *et al.* Cell-surface protein-protein interaction analysis with time-resolved FRET and snap-tag technologies: application to GPCR oligomerization. *Nature methods* **5**, 561-567, doi:10.1038/nmeth.1213 (2008).
92 Nikic, I. *et al.* Minimal tags for rapid dual-color live-cell labeling and super-resolution microscopy. *Angew Chem Int Ed Engl* **53**, 2245-2249, doi:10.1002/anie.201309847 (2014).

93 Pandy-Szekeres, G. *et al.* GPCRdb in 2018: adding GPCR structure models and ligands. *Nucleic Acids Res* **46**, D440-D446, doi:10.1093/nar/gkx1109 (2018).
94 Isbilir, A., Moller, J., Bock, A., Zabel, U., Annibale, P., Lohse M.J. Visualization of class A GPCR oligomerization by image-based fluorescence fluctuation spectroscopy. *biorXiv*, doi:https://doi.org/10.1101/240903 (2017).
95 Arai, R., Ueda, H., Kitayama, A., Kamiya, N. & Nagamune, T. Design of the linkers which effectively separate domains of a bifunctional fusion protein. *Protein engineering* **14**, 529-532 (2001).
96 Fricke, F., Beaudouin, J., Eils, R. & Heilemann, M. One, two or three? Probing the stoichiometry of membrane proteins by single-molecule localization microscopy. *Scientific reports* **5**, 14072, doi:10.1038/srep14072 (2015).
97 Latty, S. L. *et al.* Referenced Single-Molecule Measurements Differentiate between GPCR Oligomerization States. *Biophys J* **109**, 1798-1806, doi:10.1016/j.bpj.2015.09.004 (2015).
98 Bhatia, S., Edidin, M., Almo, S. C. & Nathenson, S. G. Different cell surface oligomeric states of B7-1 and B7-2: implications for signaling. *Proceedings of the National Academy of Sciences of the United States of America* **102**, 15569-15574, doi:10.1073/pnas.0507257102 (2005).
99 Kraetke, O. *et al.* Dimerization of corticotropin-releasing factor receptor type 1 is not coupled to ligand binding. *JRecept Signal Transduct Res* **25**, 251-276, doi:MHP405M576386611 [pii]
10.1080/10799890500468838 (2005).
100 Teichmann, A. *et al.* The specific monomer/dimer equilibrium of the corticotropin-releasing factor receptor type 1 is established in the endoplasmic reticulum. *JBiol Chem* **289**, 24250-24262, doi:10.1074/jbc.M114.553644 (2014).
101 Moller, T. C. *et al.* Oligomerization of a G protein-coupled receptor in neurons controlled by its structural dynamics. *Scientific reports* **8**, 10414, doi:10.1038/s41598-018-28682-6 (2018).
102 Trullo, A., Corti, V., Arza, E., Caiolfa, V. R. & Zamai, M. Application limits and data correction in number of molecules and brightness analysis. *Microscopy research and technique* **76**, 1135-1146, doi:10.1002/jemt.22277 (2013).
103 Digman, M. A. *et al.* Measuring fast dynamics in solutions and cells with a laser scanning microscope. *Biophys J* **89**, 1317-1327, doi:10.1529/biophysj.105.062836 (2005).
104 D'Agostino, R. B. S. M. *Goodness-Of-Fit Techniques*. (Marcel Dekker, New York, 1986).
105 Ulbrich, M. H. & Isacoff, E. Y. Subunit counting in membrane-bound proteins. *Nature methods* **4**, 319-321, doi:10.1038/nmeth1024 (2007).
106 Jonas, K. C., Huhtaniemi, I. & Hanyaloglu, A. C. Single-molecule resolution of G protein-coupled receptor (GPCR) complexes. *Methods in cell biology* **132**, 55-72, doi:10.1016/bs.mcb.2015.11.005 (2016).
107 Serfling, R., Seidel, L., Bottke, T. & Coin, I. Optimizing the Genetic Incorporation of Chemical Probes into GPCRs for Photo-crosslinking Mapping and Bioorthogonal Chemistry in Live Mammalian Cells. *JVis Exp*, doi:10.3791/57069 (2018).
108 Balleza, E., Kim, J. M. & Cluzel, P. Systematic characterization of maturation time of fluorescent proteins in living cells. *Nature methods* **15**, 47-51, doi:10.1038/nmeth.4509 (2018).

109 Rizzo, M. A., Springer, G. H., Granada, B. & Piston, D. W. An improved cyan fluorescent protein variant useful for FRET. *Nat Biotechnol* **22**, 445-449, doi:10.1038/nbt945 (2004).
110 Goedhart, J. *et al.* Structure-guided evolution of cyan fluorescent proteins towards a quantum yield of 93%. *Nat Commun* **3**, 751, doi:10.1038/ncomms1738 (2012).
111 Ormo, M. *et al.* Crystal structure of the Aequorea victoria green fluorescent protein. *Science* **273**, 1392-1395, doi:10.1126/science.273.5280.1392 (1996).
112 Kremers, G. J., Goedhart, J., van Munster, E. B. & Gadella, T. W., Jr. Cyan and yellow super fluorescent proteins with improved brightness, protein folding, and FRET Forster radius. *Biochemistry* **45**, 6570-6580, doi:10.1021/bi0516273 (2006).
113 Bajar, B. T. *et al.* Improving brightness and photostability of green and red fluorescent proteins for live cell imaging and FRET reporting. *Scientific reports* **6**, 20889, doi:10.1038/srep20889 (2016).
114 Shaner, N. C. *et al.* A bright monomeric green fluorescent protein derived from Branchiostoma lanceolatum. *Nature methods* **10**, 407-409, doi:10.1038/nmeth.2413 (2013).
115 Shen, Y., Chen, Y., Wu, J., Shaner, N. C. & Campbell, R. E. Engineering of mCherry variants with long Stokes shift, red-shifted fluorescence, and low cytotoxicity. *PloS one* **12**, e0171257, doi:10.1371/journal.pone.0171257 (2017).
116 Bindels, D. S. *et al.* mScarlet: a bright monomeric red fluorescent protein for cellular imaging. *Nature methods* **14**, 53-56, doi:10.1038/nmeth.4074 (2017).
117 Herrick-Davis, K. & Mazurkiewicz, J. E. Fluorescence correlation spectroscopy and photon-counting histogram analysis of receptor-receptor interactions. *Methods in cell biology* **117**, 181-196, doi:10.1016/B978-0-12-408143-7.00010-4 (2013).
118 Stoneman, M. R. *et al.* A general method to quantify ligand-driven oligomerization from fluorescence-based images. *Nature methods* **16**, 493-496, doi:10.1038/s41592-019-0408-9 (2019).

Generating fluorescent GPCR constructs (Step 1)

GPCR labeled construct

t=1-1.5 weeks

Step 1, Option A
Figure 2A-B

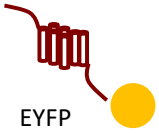

Pause point.

Step 1, Option B
Figure 3C

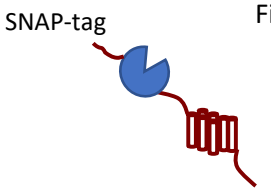

Pause point.

Step 1, Option C
Figure 3D

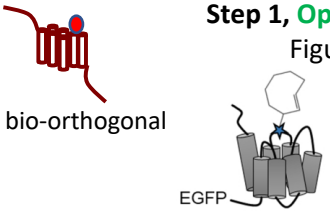

Pause point.

Sample preparation and labeling (Step 2)

Option A

Steps 2.I-II: Transfect. Cells should appear as in Figure 2 A-B after 24-48h

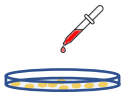

Steps 2.IV-VII: Label for 30'. Cells should look like Figure 2C

Option B

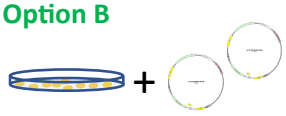

Step 2. I-VI: Transfect (+MbPylRSAF/4xtRNAM15). Wait 24h

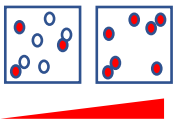

Step 2 VII-VIII: Label 10'. Cells should look like Figure 2E-H. Dye titration yields monomer control as in Figure 3D

Optional. Quantify labeling efficiency according to the steps described in Box 1

Data acquisition (Steps 3-9)

Steps 3-8: Setup confocal acquisition

- Detector Calibration (Box 2)
- Pixel size/Scan Rate/ Excitation and emission wavelengths
- Mount sample
- Find cells

Option A Step 9. I-V: temporal brightness as in Figure 4

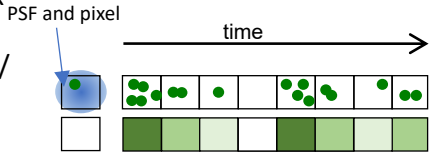

average *k* photons, variance σ^2

Pause point.

t=6 h

Option B Step 9. I-V: spatial brightness as in Figure 5

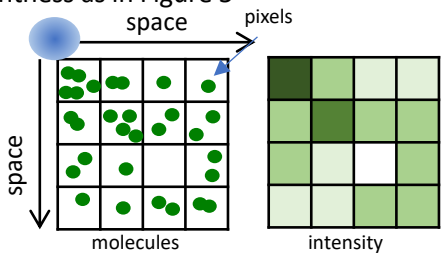

t=3 h

Data analysis and interpretation (Steps 10-14)

Step 10-11: load data into IgorPro (or other software of choice)

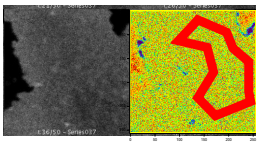

Steps 12: Analysis of datasets

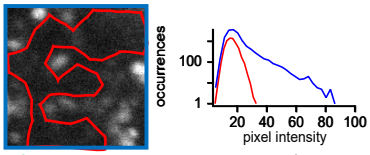

Option A: Step 12. I-IV Optimize area selection for TB acquisition as in Figure 4D-H and Figure 6

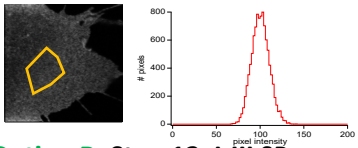

Option B: Step 12. I-III SB. Optimize area selection of SB as in Figures 5-6

t=3 h t=3 h t=3 h

Step 13-14 Gather data from cells. Generate SB vs TB 2D map as in Figure 7A-B

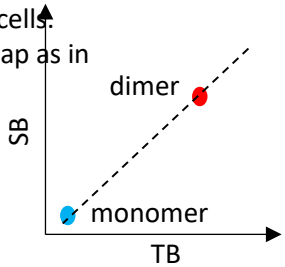

t=1 day

Box 1 (only for dual labeled samples) (as in Figure 2E-F): sequential dual color acquisition and analysis

N values from two labels as scatter (Figure 8A-B)

t=1 day

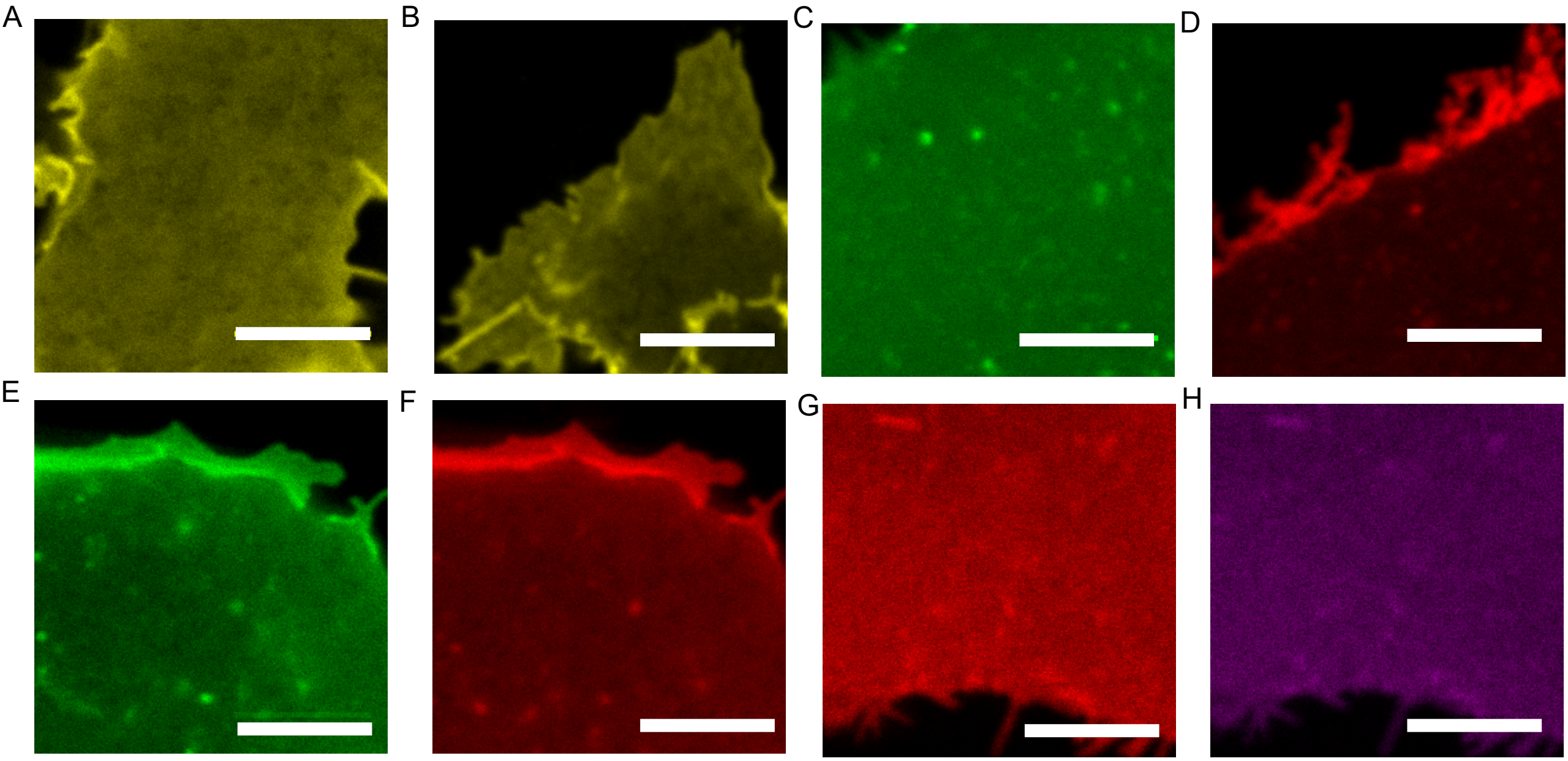
A
B
C
D
E
F
G
H

A

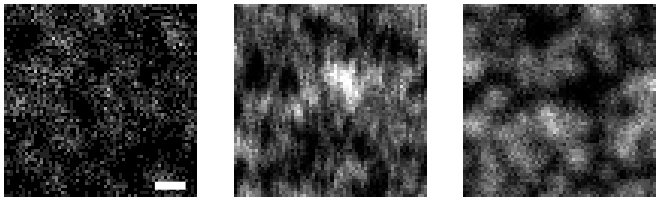

	Apparent Brightness
0.5 $\mu m^2/s$ 3D	5,7
0.5 $\mu m^2/s$ 2D	6,8
0.01 $\mu m^2/s$ 2D	4,4

B

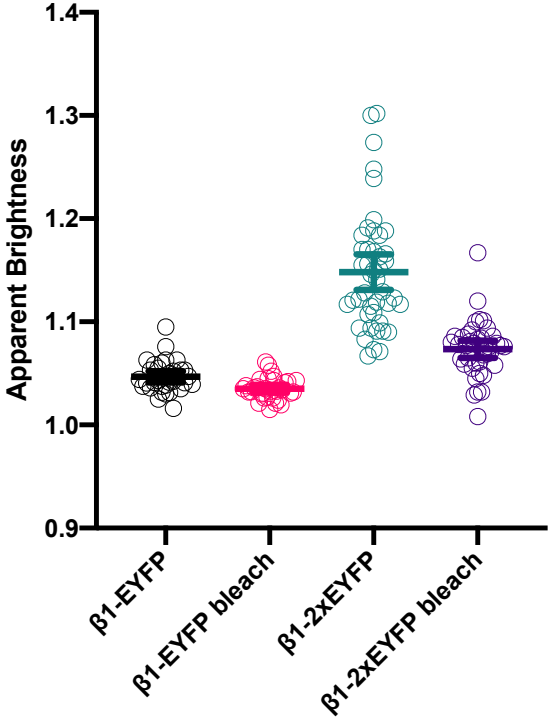

C

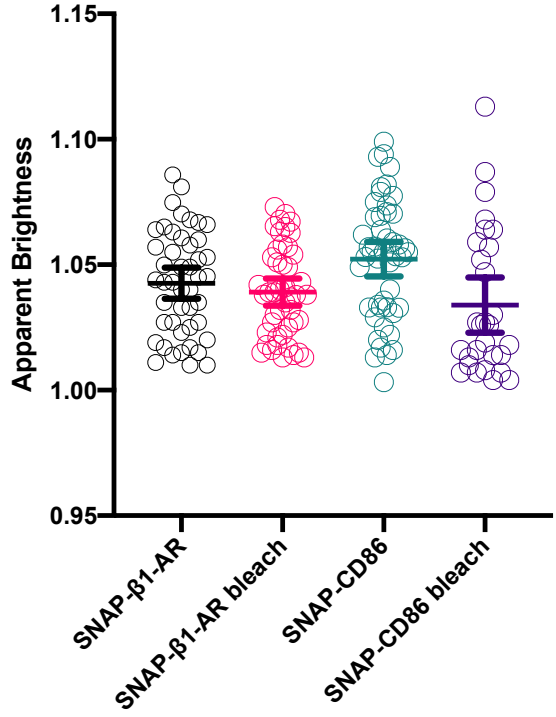

D

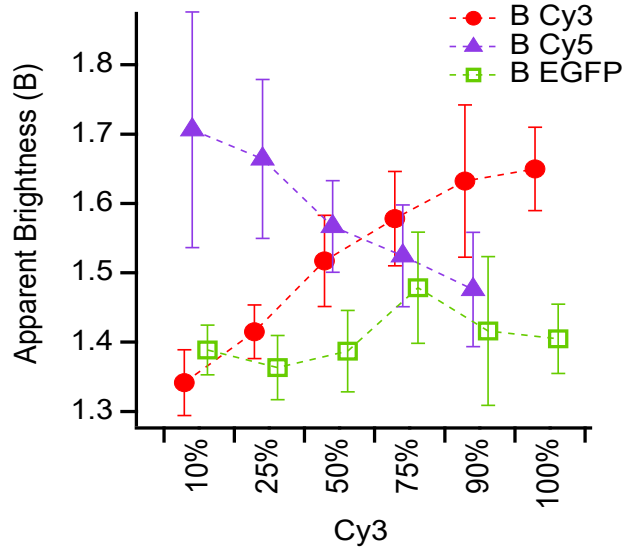

A

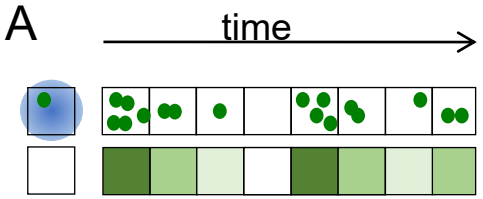

Apparent brightness (B) $B = \frac{\#^{\$}}{\%} = 1 + \epsilon$

Emitters per pixel (N) $N = \frac{k}{\epsilon}$

average *k* photons, variance σ^2

B

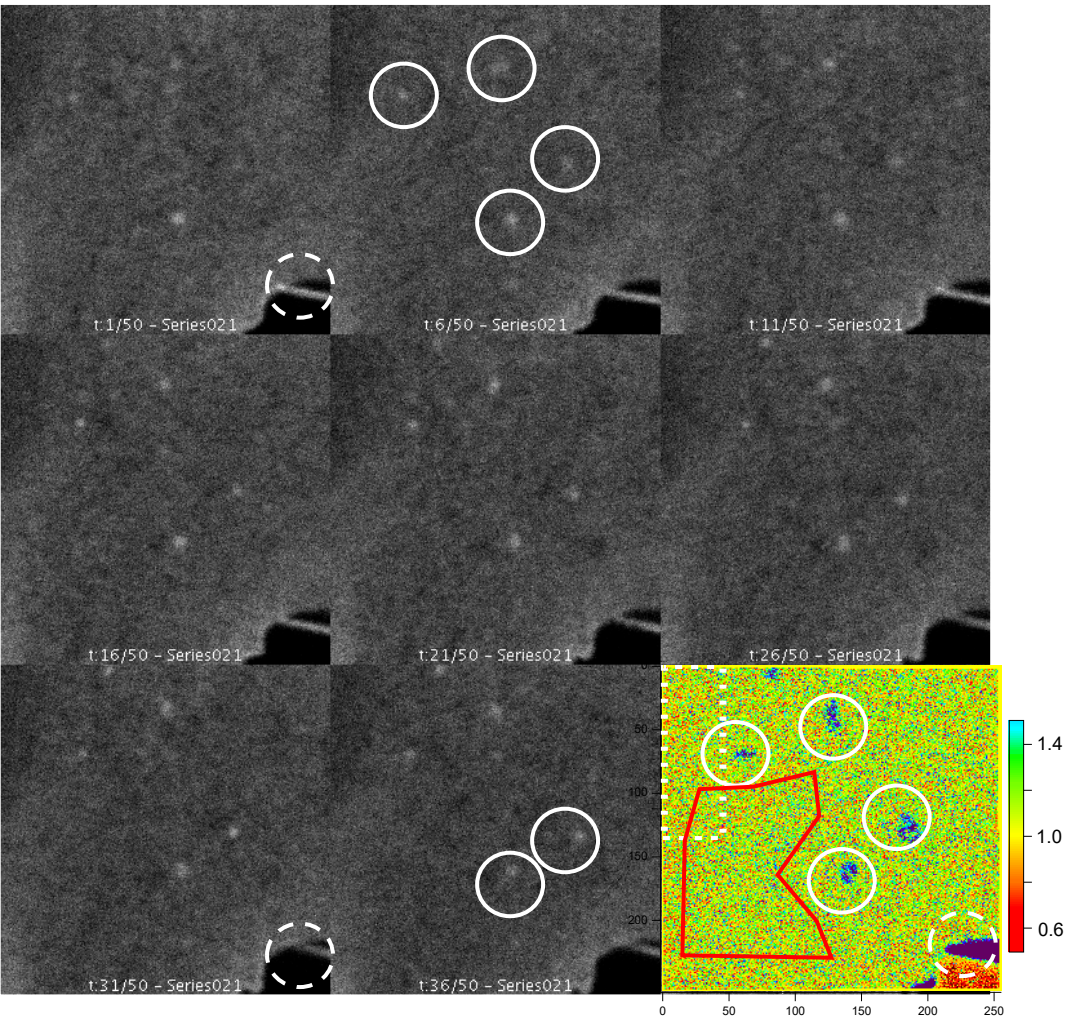

C

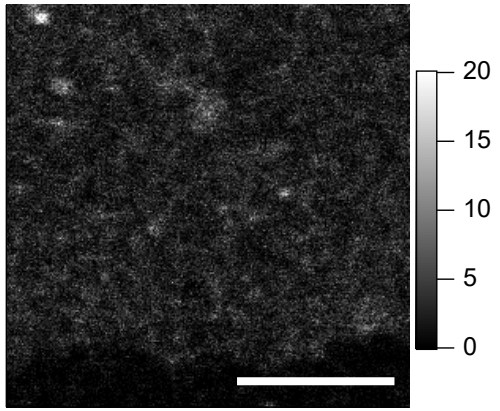

D

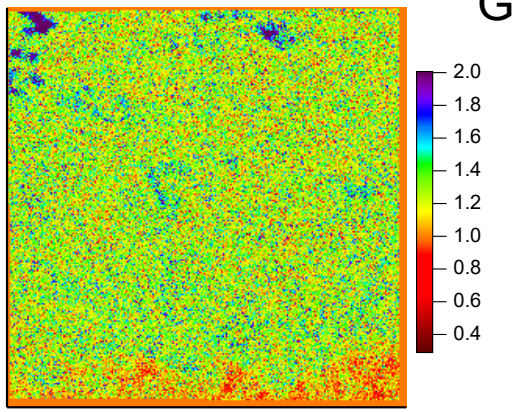

E

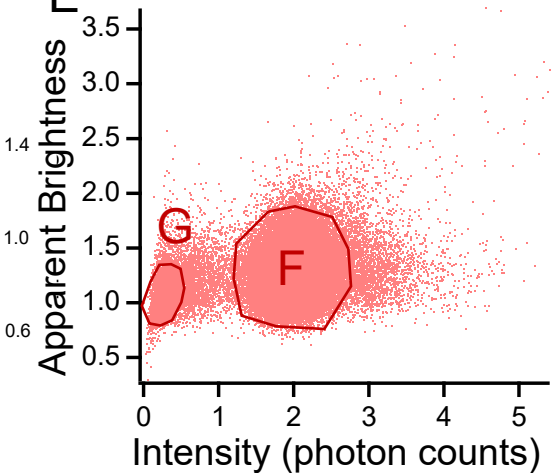

F

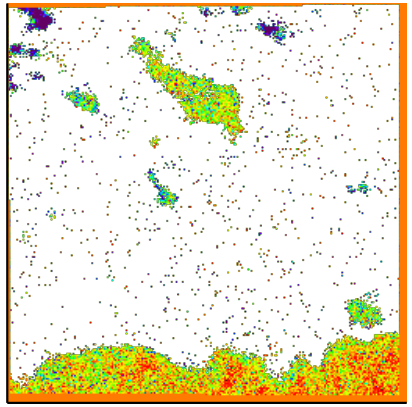

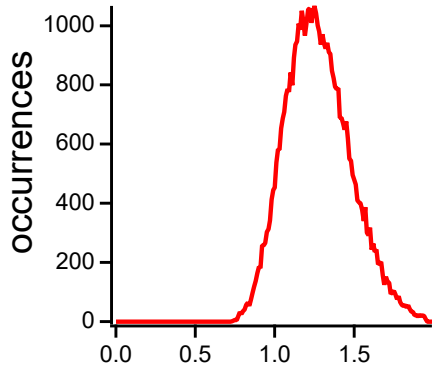

G

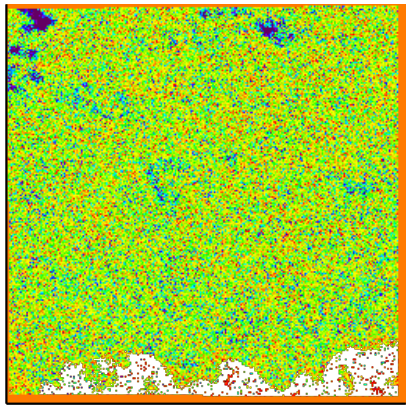

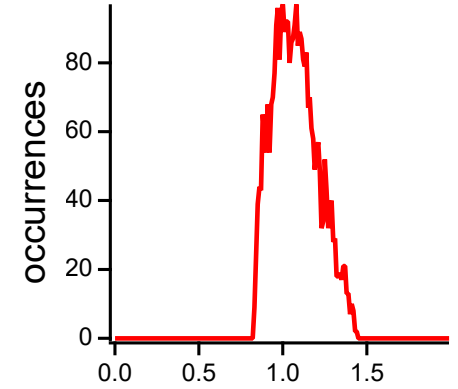

H

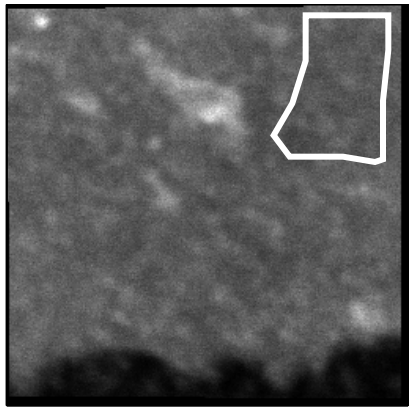

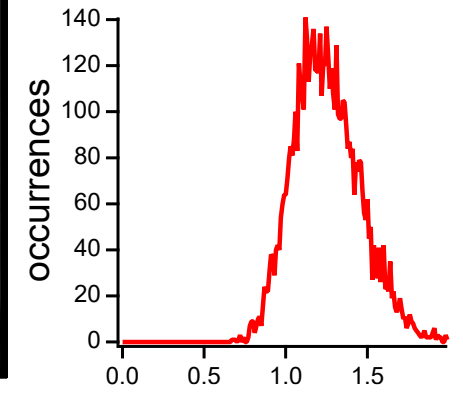

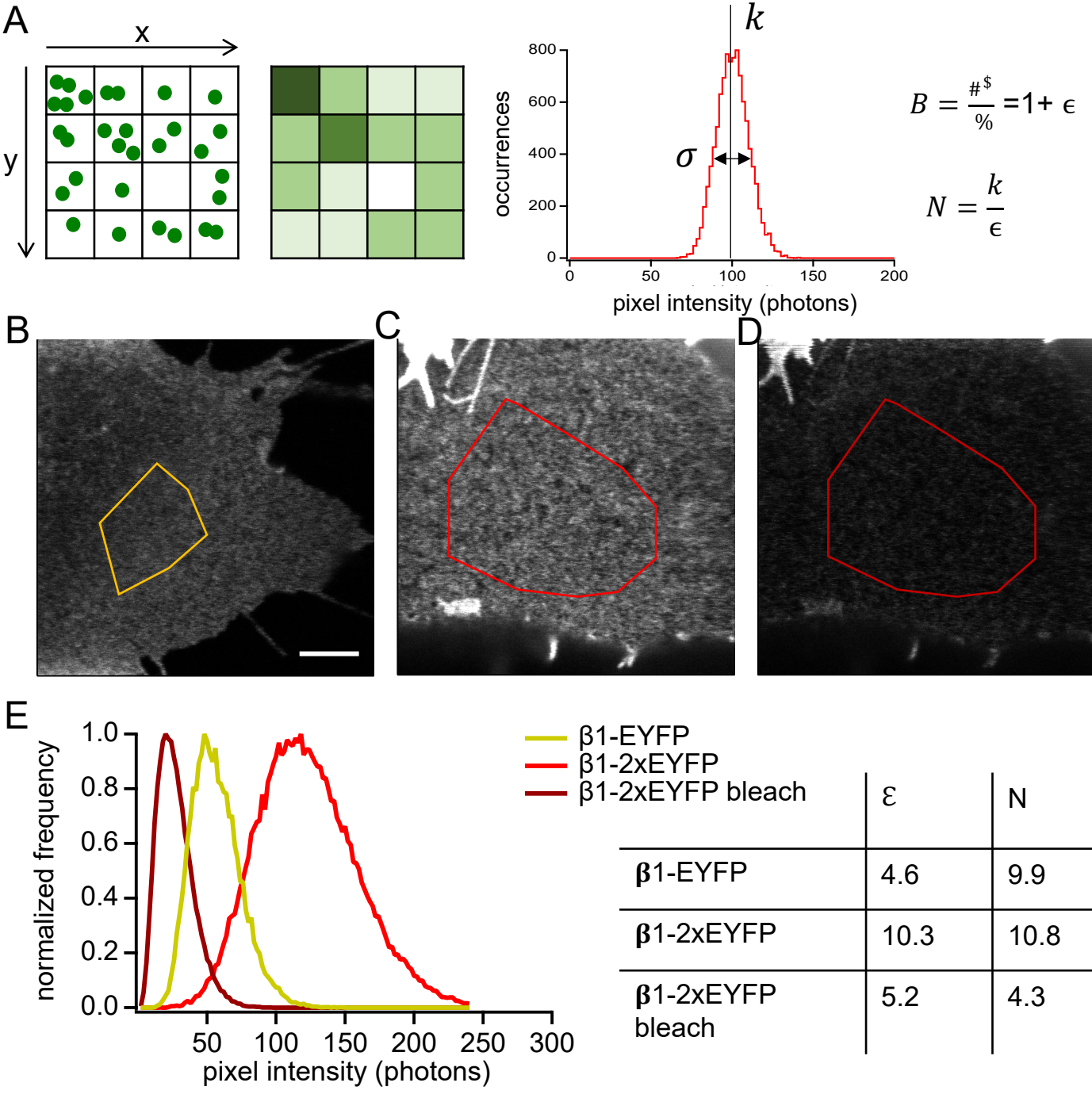

	ε	N
β1-EYFP	4.6	9.9
β1-2xEYFP	10.3	10.8
β1-2xEYFP bleach	5.2	4.3

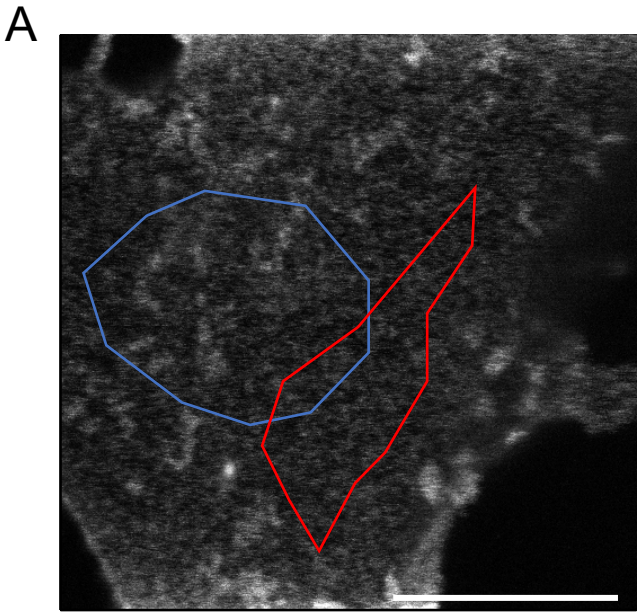

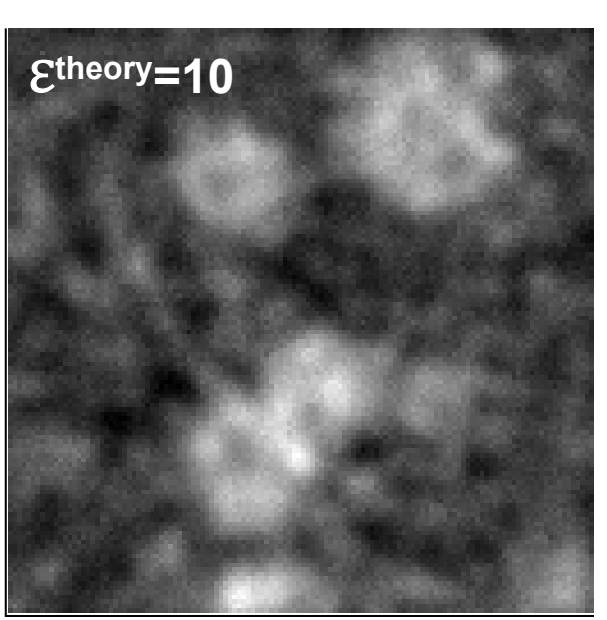

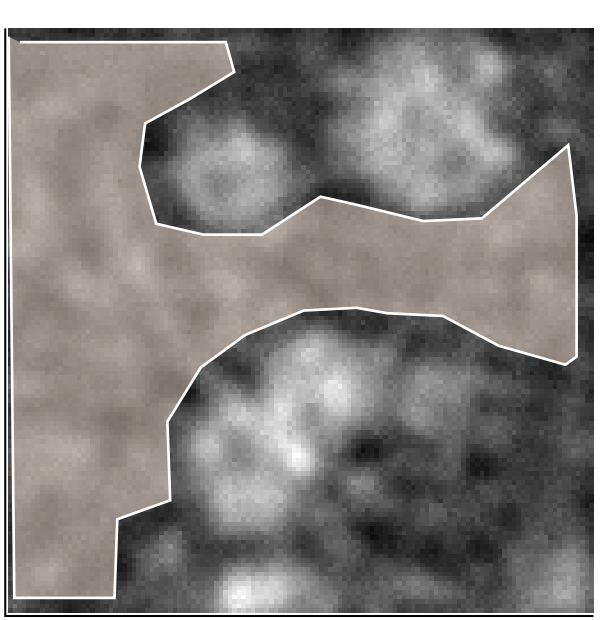

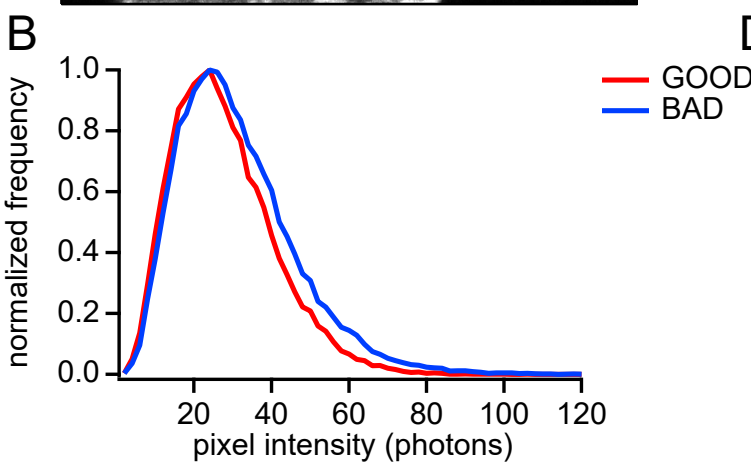

	ε	N
GOOD	4.9	5.4
BAD	6.3	4.8

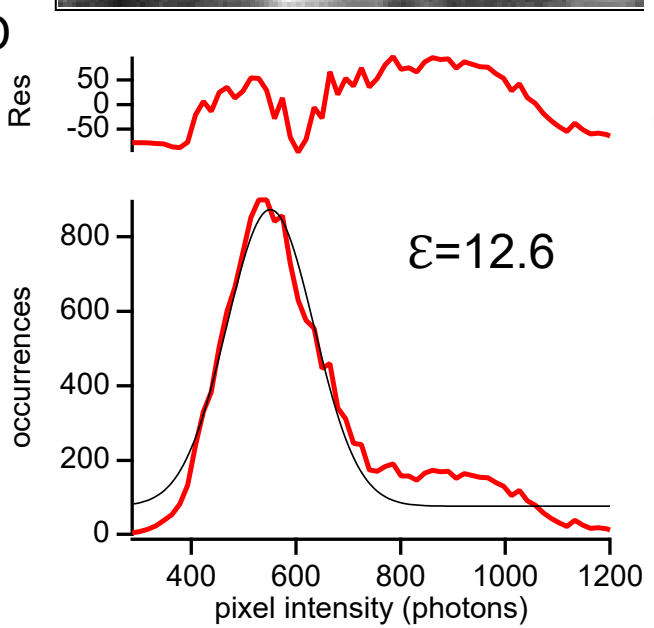

Kolmogorov Smirnov Gaussianity test score 0.07

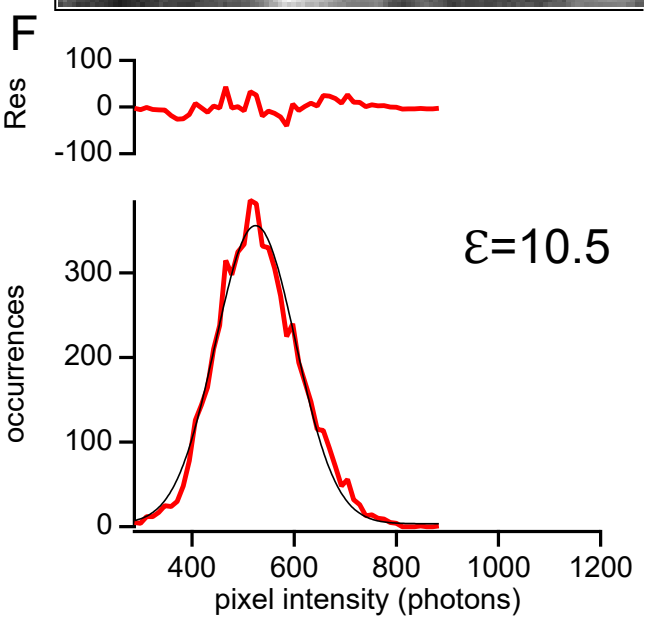

Kolmogorov Smirnov Gaussianity test score 0.53

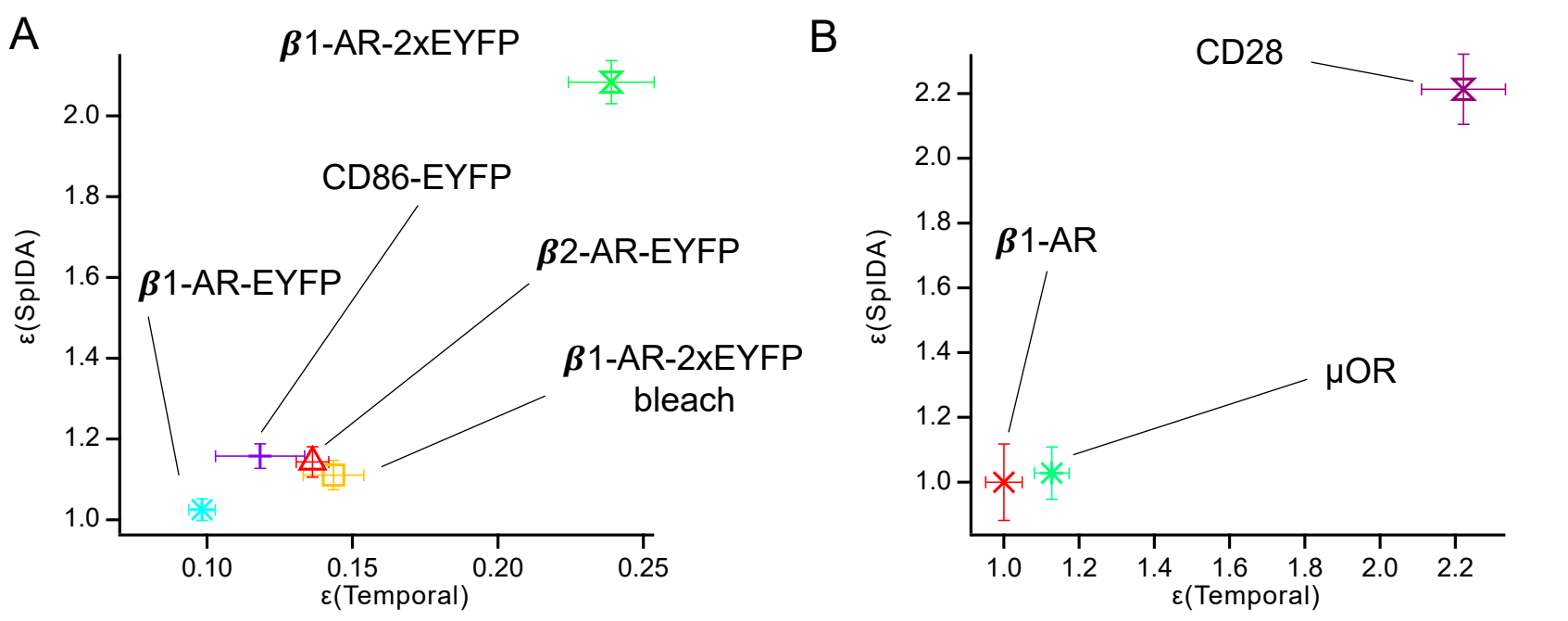
A
β1-AR-2xEYFP
CD86-EYFP
β2-AR-EYFP
β1-AR-EYFP
β1-AR-2xEYFP
bleach
ε(SpIDA)
ε(Temporal)
2.0
1.8
1.6
1.4
1.2
1.0
0.10
0.15
0.20
0.25
B
CD28
β1-AR
μOR
ε(SpIDA)
ε(Temporal)
2.2
2.0
1.8
1.6
1.4
1.2
1.0
1.0
1.2
1.4
1.6
1.8
2.0
2.2

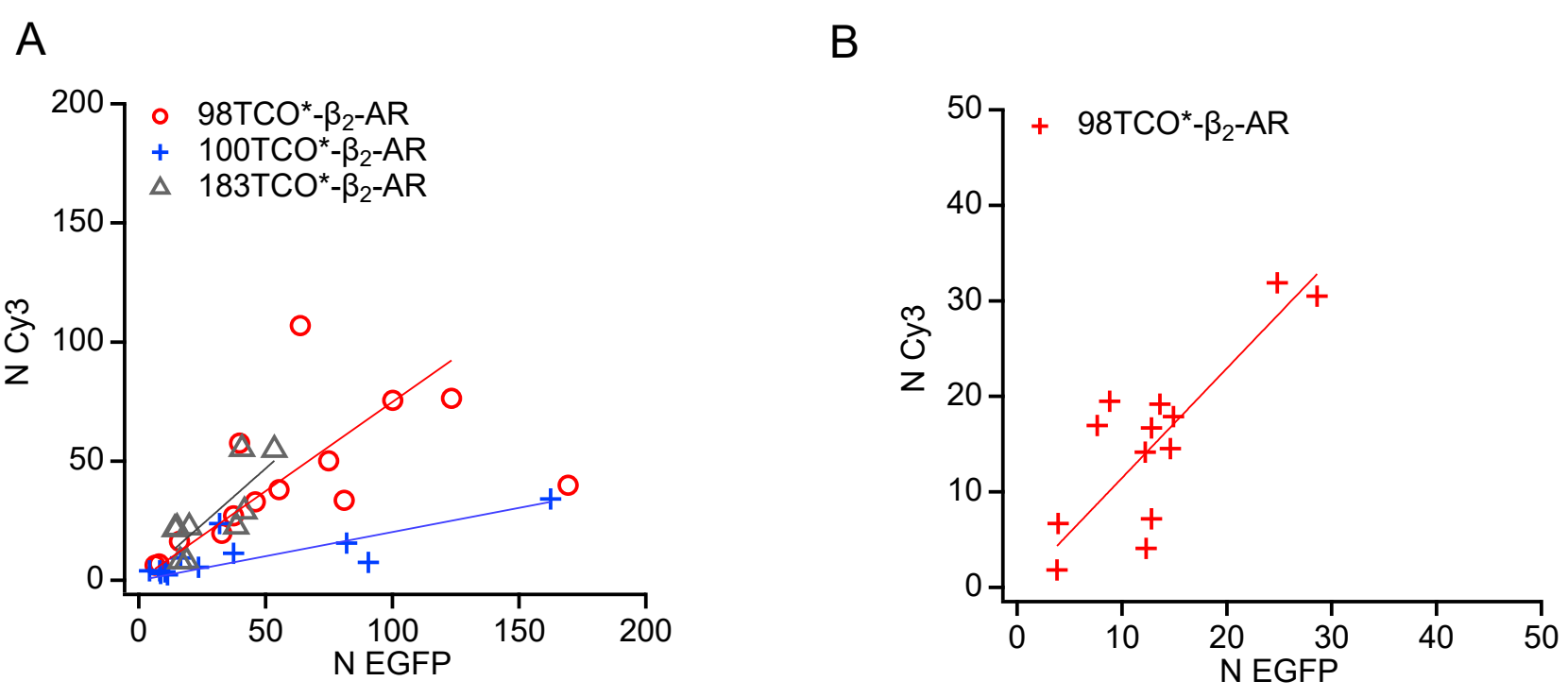
A
98TCO*-β2-AR
100TCO*-β2-AR
183TCO*-β2-AR
N Cy3
N EGFP
0
50
100
150
200
B
98TCO*-β2-AR
N Cy3
N EGFP
0
10
20
30
40
50

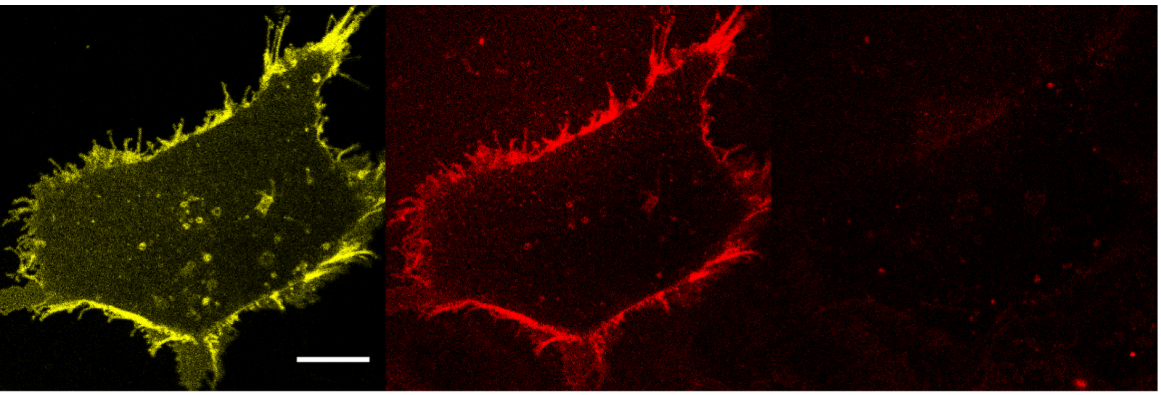

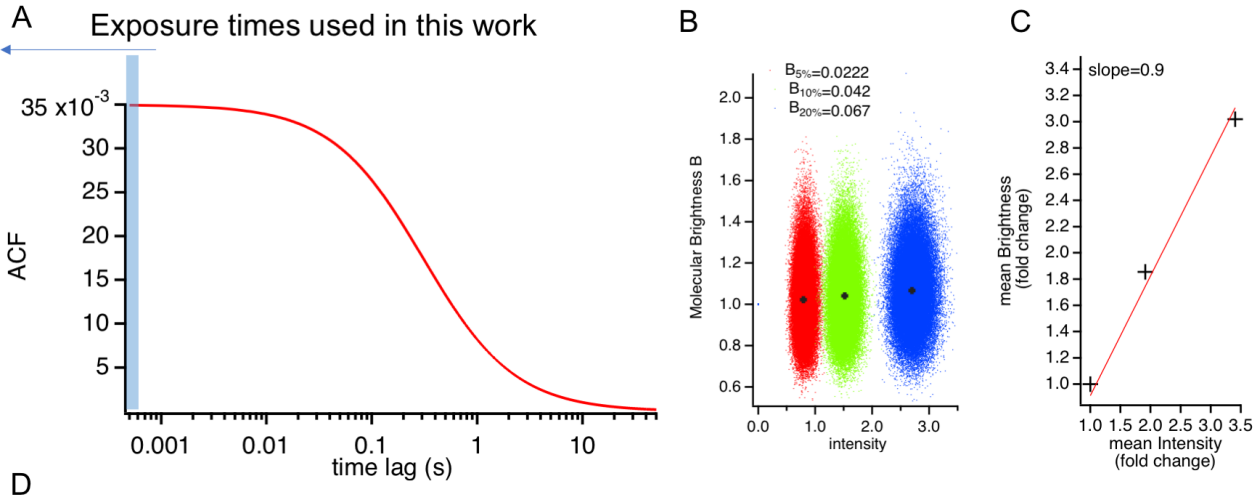
A
Exposure times used in this work
35 x10-3
30
25
20
15
10
5
ACF
0.001
0.01
0.1
1
10
time lag (s)
B
B5%=0.0222
B10%=0.042
B20%=0.067
Molecular Brightness B
2.0
1.8
1.6
1.4
1.2
1.0
0.8
0.6
0.0
1.0
2.0
3.0
intensity
C
slope=0.9
mean Brightness
(fold change)
3.4
3.2
3.0
2.8
2.6
2.4
2.2
2.0
1.8
1.6
1.4
1.2
1.0
1.0 1.5 2.0 2.5 3.0 3.5
mean Intensity
(fold change)
D
Photon Counting HyD
occurrences
counts
Koff=352
σ0=14
S=501
Analog PMT (gain=800)
occurrences
counts

A Image export

B N & B processing

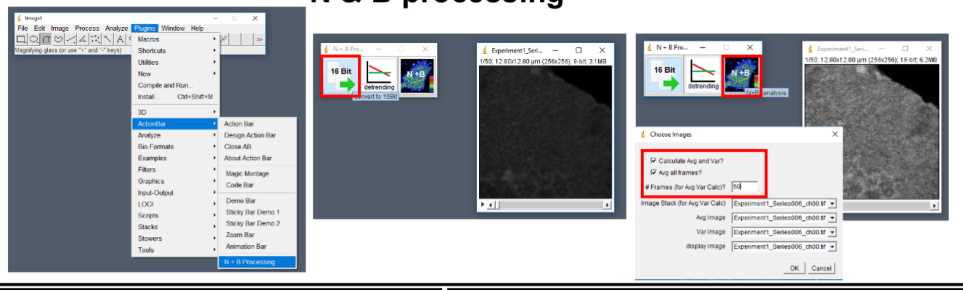

C 2D histogram and ROI

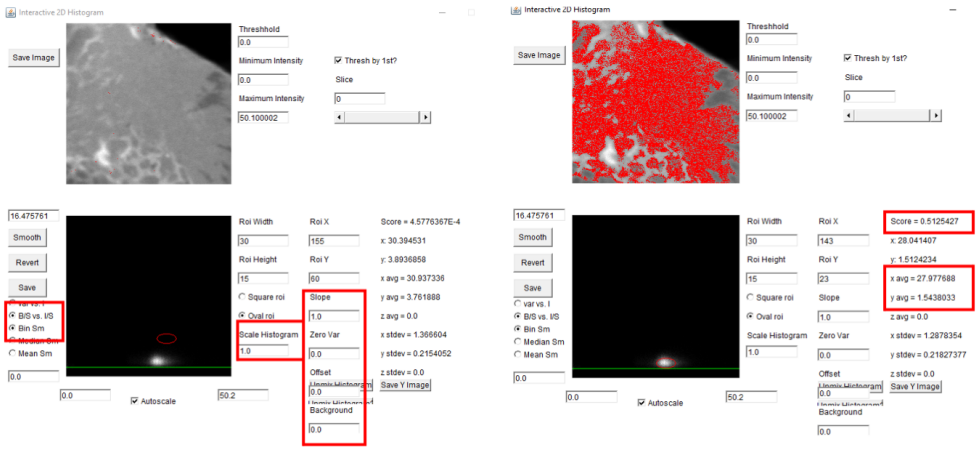

D Data fitting

$$N = \frac{I}{\varepsilon} = \frac{I}{B-1} = \frac{"x\ avg"}{"y\ avg"-1}$$

	EGFP (Ch00) Apparent Brightness (avg y)	Intensity (avg x)	Number of emitters	Cy3 (Ch01) Brightness (avg y)	Intensity (avg x)	Number of emitters
Series 004	1.225	7.822	34.789	1.432	16.554	38.290
Series 005	1.167	6.650	39.756	1.518	15.537	30.013
Series 006	1.309	23.101	74.847	1.609	56.035	92.003
Series 007	1.289	15.721	54.363	1.635	31.701	49.923
Series 008	1.145	5.243	36.254	1.487	10.839	22.260
Series 009	1.202	10.118	49.975	1.474	22.811	48.090
Series 010	1.237	8.570	36.089	1.571	17.094	29.919